MONTHLY NOTICES

OF THE

ROYAL ASTRONOMICAL SOCIETY

Vol. 103 No. 4

MEETING OF 1943 JUNE 11

Professor E. A. Milne, President, in the Chair

The election by the Council of the following Fellows was duly confirmed:—

Albert Edward Carter, 30 Primrose Hill, Bath, Somerset;
Ernest Edwin Perrin, M.Sc., 38 Lime Tree Grove, Shirley, Croydon, Surrey;
Richard Griffith Quirk, A.I.N.A., 23 Eden Quay, Dublin; and
Lieutenant George Cecil Losh Saul, R.N.R. (retired), F.R.E.S., A.I.N.A., 12 Manor Road, Beckenham, Kent.

The following candidates were proposed for election as Fellows of the Society, the names of the proposers from personal knowledge being appended:—

Rev. Harold William Heaslip, 32 Orlando Street, Stratford, New Zealand (proposed by C. E. Adams);
Flying-Officer Paul Ledoux, c/o Royal Astronomical Society, Burlington House, London, W. 1 (proposed by H. H. Plaskett);
John Walter Ryde, F.Inst.P., Research Laboratories of the General Electric Co. Ltd., Wembley, Middlesex (proposed by D. H. Sadler);
Karai Sivachidambara Mahesa Sarma, Notary Public, Pulavar House, Karainagar, Ceylon (proposed by A. P. Kandasamy); and
Frank Sheldrake, B.Sc., 43 Victoria Road, Sheffield, 10 (proposed by Reginald R. S. Cox).

Thirty-seven presents were announced as having been received since the last ordinary meeting, including:—

New York Federal Works Agency: Works Projects Administration Tables: Miscellaneous Physical Tables. Planck's Radiation Functions and Electronic Functions (presented by the National Bureau of Standards).
F. Berthoud, Traité des Horloges Marines (presented by W. H. Owston).
——, De la Mesure du Temps (presented by W. H. Owston).
——, Les Longitudes par la Mesure du Temps (presented by W. H. Owston).

The President invited Fellows to join him in congratulating the Astronomer Royal, Sir Harold Spencer Jones, on the honour of Knighthood conferred upon him by His Majesty the King.

MEETING OF 1943 JULY 9

Professor E. A. Milne, President, in the Chair

The election by the Council of the following Fellow was duly confirmed:—

Polydore Swings, 975 E. Green Street, Pasadena, Cal., U.S.A.

The following candidates were proposed for election as Fellows of the Society, the name of the proposer from personal knowledge being appended:—

Dana Kavanagh Bailey, B.S., M.A., 3902 Spuyten Duyvil Parkway, New York City, U.S.A. (proposed by T. L. Eckersley);

Howard Laurence Kelly, A.R.I.B.A., 44 Gilda Court, Watford Way, London, N.W. 7 (proposed by G. E. Patston); and

Gunnar Randers, 18 Gloucester Road, London, S.W. 7 (proposed by A. S. Eddington).

Thirty-two presents were announced as having been received since the last meeting, including:—

H.M. Nautical Almanac Office: Apparent Places of Fundamental Stars, 1944 (presented by H.M. Stationery Office).

The President announced that the Council had decided that the Bye-laws 26A and 26B should be interpreted as conceding the following privileges to Fellows excused their annual contributions under these two Bye-laws:—

(i) Of assuming the title of Fellow of the Society;
(ii) Of attending Ordinary Meetings and Annual General Meetings of the Society;
(iii) Of using the rooms of the Society and consulting the library, but not of borrowing books from the library;

but that they shall have no other privileges.

The President further announced that Professor S. Rosseland would deliver the George Darwin Lecture at the Ordinary Meeting of the Society on 1943 September 10 and had chosen as his subject "The Pulsation Theory of Cepheid Variables."

SPECTROGRAPHIC OBSERVATIONS AT THE TOTAL SOLAR ECLIPSE OF 1940 OCTOBER 1

III. THE SPECTRUM OF THE EXTREME LIMB OF THE SUN

R. O. Redman

(Received 1943 May 28)

Summary

(1) A preliminary examination of the spectrum of the extreme limb of the Sun, photographed with a large slit spectrograph immediately after third contact at the 1940 eclipse, showed that it is essential to remove the superposed chromospheric spectrum before any significant results with regard to the spectrum just within the limb can be deduced.

(2) A method of performing this correction was devised, and the corrected spectrum, arising from less than one second of arc within the limb, at $\cos\theta = 0{\cdot}05$, was found to contain few, if any, emission lines, excepting the hydrogen Balmer series. It is shown that the true change from an emission to an absorption spectrum must have been scanned by the Moon's limb in not more than two seconds of time, possibly in less than one second. To study the transition in detail, as had originally been intended, is therefore a much more difficult problem than hitherto supposed, and cannot be profitably attempted with these spectrograms.

(3) Measures of the equivalent widths of 251 lines showed that at $\cos\theta = 0{\cdot}05$ weak lines are as strong, or slightly stronger, than at the centre of the disk. Lines of equivalent width exceeding about 0·13 A. are weakened at the limb, the weakening increasing with equivalent width.

(4) An examination of ordinary Fraunhofer line theory failed to reveal any combination of parameters which would explain this result. It is suggested that the clue to this puzzle lies in a roughness of the Sun's surface, probably associated with the solar granulation, which in effect reduces the value of θ for observations near the limb. Quantitative estimates show that an apparent $\cos\theta = 0{\cdot}05$ may be increased to an effective $\cos\theta = 0{\cdot}20$ in this manner, while an apparent $\cos\theta = 0{\cdot}3$ may be increased to 0·39.

(5) Accepting a correction to θ of this order, a modified Schuster-Schwarzschild model is suggested, which within present observational uncertainties fits reasonably well (*a*) the eclipse observations, (*b*) Miss Adam's observations of weak lines, (*c*) Houtgast's observations of strong lines of *Fe*I and *Ca*I. Until more accurate values for the intensity of emission in the continuous spectrum as a function of optical depth are available, and until we have discovered more about the effect of the roughness of the Sun's surface upon centre-limb changes in the spectrum, closer quantitative comparison of theory with observation appears to be premature.

Two papers describing respectively the observational procedure at the 1940 eclipse and some results concerning the chromospheric spectrum have already been published.* Following the work on the emission lines, attention was turned to the Fraunhofer spectrum at the extreme limb of the Sun, concentrating chiefly on the second of the

* *M.N.*, 102, 134, 140, 1942.

two eclipse plates. This was earlier described in the following words, which may profitably be repeated here: "Exposure 1 has an excellent example of low chromospheric spectrum, but no absorption lines other than self-reversals which remain above the level of the continuous. On exposure 2 we have Fraunhofer spectrum from the extreme limb. The continuous spectrum is considerably stronger than on 1, with nearly four hundred identifiable absorption lines. Emission lines are still very numerous, but the fainter of them are not so easily picked out as on the first exposure. Subsequent exposures show a continuous spectrum quickly increasing in strength, with Fraunhofer lines becoming much more numerous, as well as stronger individually, and the emission lines relatively less conspicuous, although there are many still to be seen on the edges even of exposure 10." The chief purpose for which these observations were made was to study the transition from the emission spectrum of the chromosphere to the Fraunhofer spectrum of the disk, of which there appeared to be a good record on this plate. The importance of this transition in relation to the theory of formation of Fraunhofer lines was emphasized by Woolley when discussing observations made at the earlier eclipse of 1936, "as the conditions are very critical and will show up weaknesses in a mathematical representation which will do well enough when it is only used to predict contours for the middle of the solar disk, or for a star as a whole." *

A first tentative attack on the question was made by examining the lines of multiplets, chiefly of *Fe*I, on exposure 2. The results were not very satisfactory and ultimately the writer became convinced that before continuing it would be necessary to remove, if possible, the superposed chromospheric spectrum. The exposures had been made at third contact, with the image of the solar disk held as closely as possible tangential to the spectrograph slit. Under perfect conditions the image would have shown a very thin crescent, with the chromosphere on one side and the Moon's limb on the other.

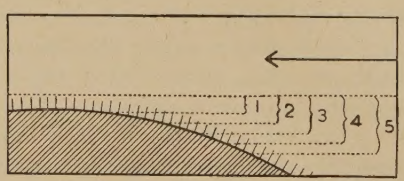

FIG. 1.—*Diagram to illustrate the regions of disk and chromosphere covered by successive exposures on Plate 2. The arrow indicates the direction of the line of sight. The vertical scale has been much exaggerated for clarity.*

The maximum width of the crescent, for exposure 10, was about 5 seconds of arc, if we consider the disk only and ignore the chromosphere. In actual fact, conditions were far from perfect; the seeing was unusually bad, even by daytime standards, and it seems probable that even for the last exposure everything was blurred together, so that what passed through the centre of the slit was a good sample of light integrated over the width of the crescent, including all disk visible and all but the highest levels of the chromosphere. Certainly this must have been the case for the earlier exposures, when the crescent was considerably thinner. Confining attention to the centre of the slit, we may then regard exposure 2 as containing all the light present on exposure 1, plus an amount from that part of the disk which had been uncovered by the Moon during the time (approximately one second) between the exposures. Similarly with subsequent exposures (Fig. 1). If we measure spectrograms 1 and 2 photometrically, reducing each to a common scale in light intensity, and subtract one from the other, *i.e.* find the difference in light intensity at each individual wave-length, the result should

* *M.N.*, 98, 3, 1937.

be the light distribution in the spectrum of that part of the Sun uncovered between the first two exposures. In other words, we should in this manner be able to get the spectrum of the limb, free from chromospheric spectrum. It should be noted that this process aims at sorting out the disk and chromosphere as they lie side by side in an ideal image of the Sun, and does not remove from the disk that part of the chromosphere lying in the line of sight. We do not desire to eliminate this last, because it is supposed to be included in ordinary Fraunhofer line theory.

Needless to say, this method is simpler in principle than it is in practice. A number of difficulties may be mentioned here:

(1) The exposure times for the plate ranged from 0·52 to 0·67 seconds, being 0·59 and 0·52 seconds respectively for exposures 1 and 2. Our plate calibration, however, was for one exposure time only, so that it is necessary to apply corrections to reduce all the spectrograms effectively to the same exposure time. For this, Schwarzschild's law was assumed, *i.e.* it was supposed that the uncorrected light intensities contained a factor t^p, where t is exposure time and p a constant for the whole plate. Experiments with a similar plate emulsion gave $p = 0{\cdot}8$. Thus the light intensities from exposure 1 must be multiplied by $(0{\cdot}52/0{\cdot}59)^{0{\cdot}8} = 0{\cdot}904$ before subtracting from exposure 2. The correction is not large, and errors in p or in the assumption that Schwarzschild's law is valid should have relatively little effect. It is estimated that the correction is unlikely to be in error by more than 10 per cent. of itself, or about 1 per cent. of the actual spectrum. The procedure is not ideal, but seems to be the only one possible here. At a future eclipse it might be practicable to observe with apparatus giving exposure times of exactly equal length, or to give the plate a double calibration, one for varying exposure times as well as the usual one for varying light intensities.

(2) The final measures, derived by this differencing process, contain a double dose of plate grain and the other common sources of error in photographic photometry. This is unavoidable and we have to regard it as merely another of the practical difficulties which make the attainment of a given standard of accuracy so much more difficult in eclipse work than in ordinary observations.

(3) The method is extremely laborious. Excluding preliminary trials, nearly 40,000 microphotometer readings were needed, and there is much material on the plates still unmeasured. Should this work be repeated at some future eclipse, under more normal circumstances than hold at the time of writing, it would be worth while constructing a machine specifically for the job, especially if the spectrograms were on a still larger scale.

(4) Another difficulty, fortunately only of minor importance in this case, is that the method requires uniform sky transparency during the exposures. In regard to cloud and haze the Calvinia sky was as near perfect as any eclipse sky is ever likely to be. There may have been some irregularity, not from the transparency but from the jumpiness of the seeing, evinced not merely by the appearance of the solar image, but also by the great strength of the "shadow bands." The fairly short exposure times may not have been sufficient to smooth out altogether the variations of illumination of the cœlostat mirror, as the shadow bands passed across it. Bad seeing, however, is in one respect a boon, for it reduces the accuracy with which the solar image has to be guided on the slit.

(5) It has also to be remembered that the Moon does not halt while each exposure is being made. We are photographing a rapidly changing phenomenon with a kind of sluggish cinematograph, too slow, as we shall see later, to record all the important changes without blurring. (We here refer to a lack of resolution in *time*, not a lack of optical definition on the plate.)

Despite all difficulties, the evidence is convincing that this or some equivalent method must be followed before we can obtain the true spectrum of the solar disk very near the limb, say for $85° < \theta < 90°$, θ being, as usual, the angle between the line of sight and the normal to the Sun's surface. Fig. 2 shows a short section of spectrum as reduced

from the microphotometer tracings at 100 : 1 magnification, with individual readings at 1 mm. intervals (0·01 mm. on the plate). (*a*) is from exposure 1, and we see what has already been described, a continuous spectrum with emission lines only. (*b*) is from exposure 2, uncorrected, and there we have a continuous spectrum with a mixture of emission and absorption lines. (*c*) is the corrected exposure 2, obtained by subtracting (*a*) from (*b*). *It shows a pure Fraunhofer spectrum with no emission lines.* Not

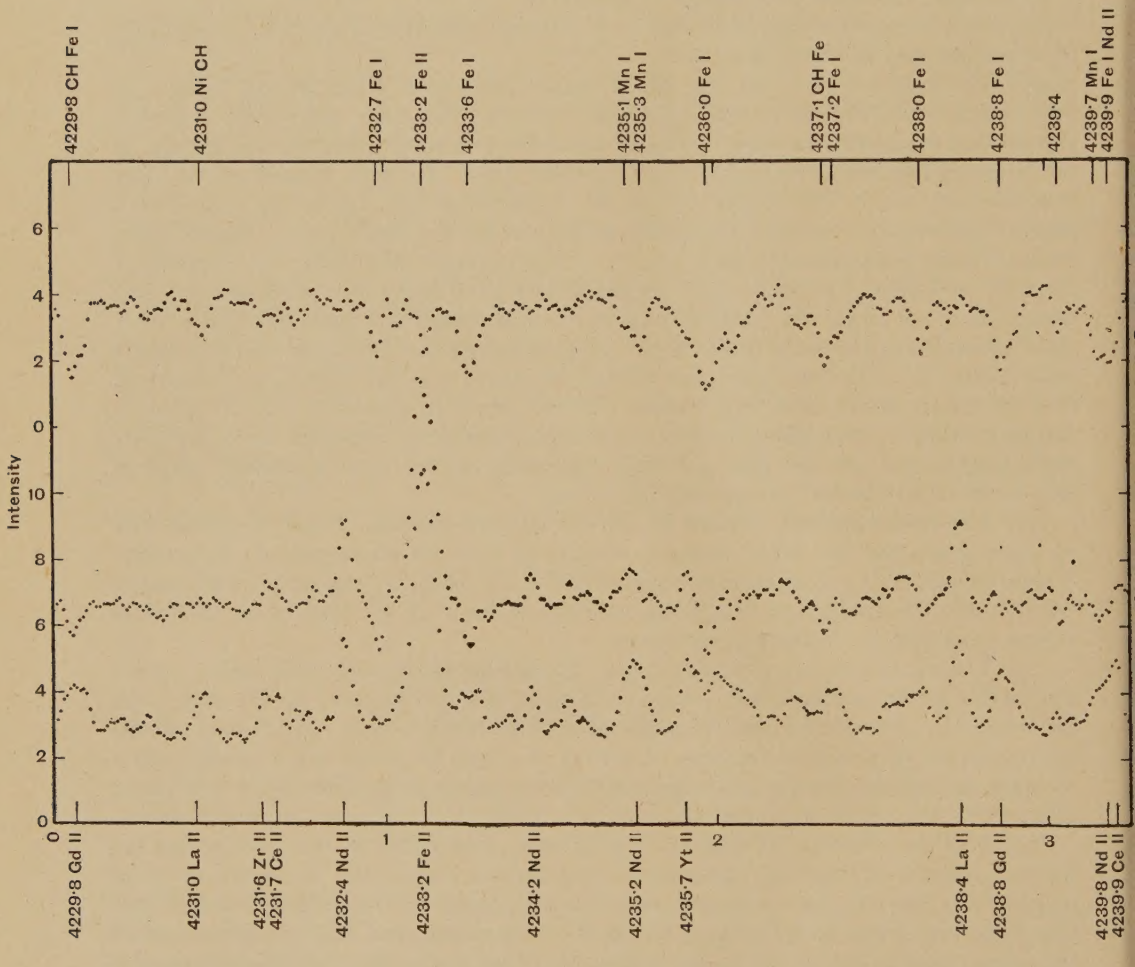

FIG. 2.—*Measured intensities from a short section of Plate 2, (a) from exposure 1, (b) from exposure 2. (c) is the corrected exposure 2, obtained by differencing (a) and (b). Computed positions of the stronger Fraunhofer lines, taken from Rowland, are at the top; of some emission lines at the bottom.*

only have the emission lines vanished, but many new Fraunhofer lines have appeared which were invisible on the uncorrected exposure 2. From their positions and intensities it is clear that these are not spurious. Almost every line of the normal solar spectrum down to Rowland number 1 can be seen, and many of Rowland number 0. Speaking more precisely, the Fraunhofer spectrum is practically complete down to equivalent width 0·020 A. In the λλ 4220–4280 region about 20 per cent. of lines of equivalent width 0·020–0·030 A. (Allen's measures) are missing. Practically the same result was obtained by differencing exposures 3 and 5, and since the list of missing lines is not

identical in the two cases, it appears that plate grain and similar irregularities are responsible and that these lines are about the faintest measurable with any certainty on these photographs. Apart from two or three of the strongest rare-earth lines, which are possibly surviving very much weakened, and the hydrogen lines, which persist as relatively weak double emission lines on an absorption line, there are no emission lines to be found on the corrected spectrum from exposure 2 over the region λλ 4100–4550. (The hydrogen lines, owing to their great strength, give less reliable results than the rest of the spectrum. With them one is obtaining a quantity of the order x by differencing two quantities of the order $10x$, measured with a light receiver, the photographic plate, whose response is of a logarithmic nature.)

One criticism may be advanced immediately, and as quickly dismissed. It may be maintained that the chromospheric spectrum is to a first approximation a reversal of the Fraunhofer spectrum, so that these results could be obtained simply by faulty overcorrection of exposure 2. Were this so, however, strong chromospheric lines would always have fairly strong absorption lines as their counterparts in the corrected spectrum. This is not the case; for example, strong rare-earth lines such as λ 4333 *La*II never show more than very weak absorption in the corrected spectrum. The correlation of line intensities in the corrected spectrum is much closer with intensities in the normal solar spectrum than with intensities in the chromospheric spectrum. We conclude that what has been obtained is really the spectrum of that part of the Sun's disk lying just within the limb, or at least is a far better approximation thereto than is the uncorrected spectrum.

Before proceeding further it is necessary to find out to what value of θ these measures refer, which entails knowing exactly where the limb of the Sun lies. The sharpness of the limb as seen in the telescope in white light is usually limited only by the seeing, and visually it appears possible to fix its position quite accurately. For instance, the semi-diameter of the Sun at unit distance is given in the *Nautical Almanac* to 0″·01, although it is true that one's confidence is a little shaken by the fact that the value used for eclipse predictions is about half a second of arc less than this, "to allow for irradiation." The limb as determined by visual observers is presumably at a place where the surface brightness of the solar image has a maximum gradient with respect to distance from the centre, and quite apart from systematic errors of measurement, whether arising from irradiation or other causes, is not necessarily the same as the limb to which theory refers. The theoretical limb is where the line of sight is tangential to the outer boundary of that part of the atmosphere forming the continuous spectrum, *i.e.* to the surface $\tau = 0$, where τ is optical depth in the continuous spectrum, measured perpendicular to the surface. How the limb of theory is situated with respect to the limb of visual observation we cannot be quite sure; probably it lies a little way outside the latter. For our purposes it has been determined by measuring the intensity in the continuous spectrum of our exposures, utilizing three wave-lengths near $H\beta$, $H\gamma$ and $H\delta$ respectively, and reducing to constant exposure time by the method described above. The maximum intensity across the width of each spectrum, or in other words the maximum when moving along the slit of the spectrograph, has been taken to be proportional to the light intensity integrated over the width of the crescent at its thickest part. It is necessary to know the darkening to the limb (although the time covered by the observations is so short that this has less effect than might at first be expected), which has been computed from the temperature distribution derived by Plaskett, as quoted by Miss Adam.* Other data were taken from the *Nautical Almanac* and the computed curve was finally fitted as well as possible to the observations (Fig. 3). Where the curve comes to intensity, zero gives us the time when the Moon's limb crossed the theoretical limb of the Sun, and this was found to be 1·1 seconds before the middle of exposure 1, or 2·1 seconds before exposure 2, which therefore relates to an average distance within the limb 0″·98. The

* *M.N.*, 100, 595, 1940.

corresponding value of cos θ is 0·045. We shall use cos $\theta = 0{\cdot}05$ in what follows. We have neglected the fact that, since the place of observation was not on the centre line of the totality belt, the slit of the spectrograph was tangential to the solar image 7° from the point of third contact, but it can be shown that to a first approximation this merely displaces the computed curve bodily along the time axis and has no appreciable effect on the estimate of θ. It has also been necessary to ignore irregularities on the Moon's limb, and the motion of the Moon during each exposure. These unavoidable complications may affect the present work in detail, but in essentials the results given below should stand. Thus we take it that *at cos* $\theta = 0{\cdot}05$ *the solar disk gives a spectrum showing Fraunhofer lines and practically no emission lines.*

One important result now appears, namely that our spectrograms are unsuitable for the original purpose for which they were taken, for it was hoped to study the transition between absorption and emission spectra in some detail, including the measurement

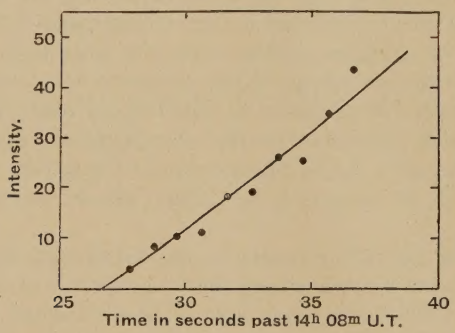

FIG. 3.—*Measured intensities in the continuous spectrum of successive exposures on Plate 2, compared with a computed curve.*

of line profiles of intermediate forms. It can now be seen that observational difficulties are much greater than was once thought, for besides being necessary to measure the photographs by an indirect method of differencing successive exposures, it is now found that the emission to absorption transition is in reality very sudden, being practically complete only one second of arc within the limb. In the circumstances in which the Calvinia observations were made the transition took place in less than 2·1 seconds of time. Furthermore, this is an upper limit and the actual change-over may be still more rapid. An inspection of the other plate, taken at second contact, suggests that it is not likely to yield very reliable information on this question, owing to irregularities of guiding, and perhaps of seeing, so that an attempt was made to obtain something further from plate 2, by measuring at some distance from the centre of the spectrograph slit. At the place selected the continuous spectrum of exposure 2 had about one-third of its intensity at the centre of the slit, and if we may take this as a guide to the value of θ, using Fig. 3, we have sin $\theta = 0{\cdot}99958$, cos $\theta = 0{\cdot}03$, the spectrum coming effectively from a place $0''{\cdot}4$ within the limb. Unfortunately the continuous spectrum on the corresponding part of exposure 1 is too weak to be measured, so that the reduction to the corrected exposure 2, carried out in the same manner as before, can be effected only fragmentarily, in those parts which are covered by fairly strong bright lines. As far as can be discovered within these limitations, the corrected spectrum still has Fraunhofer lines of about the same strength as at cos $\theta = 0{\cdot}05$, and the emission lines are still absent, or very weak (again excluding hydrogen). In other words, it is probable that at only $0''{\cdot}4$ within the limb there is still a practically pure Fraunhofer spectrum. That being so, as viewed at Calvinia the Moon's limb scanned the transition from emission to absorption in less than one second of time. It is clear that to deal with a phenomenon changing as rapidly

as this, the resolving power *in time* of an instrument able to take only one photograph per second, each exposure lasting more than half a second, is inadequate. If observations are to be made near the centre of the totality belt, as at Calvinia, a much more rapid sequence of exposures would be required, perhaps of the order of ten or a hundred per second, before the original objective could be fully attained, and this would lead to difficulty from the shadow bands, unless the seeing were unusually steady. It would probably be better to work near the edge of the totality belt, although this in turn introduces other complications, and it would also appear advantageous to use a curved slit, shaped to fit the solar image, as Dunham has suggested.

At the time when paper II was written it was believed that the exposure 2/1 was practically free of Fraunhofer spectrum and that the self-reversals and continuous spectrum seen therein were necessarily produced in the lower chromosphere. As a result of the later work just described it appears that this is probably not true, that there is still a fair amount of Fraunhofer spectrum on this first exposure, and that the self-reversals are not reversals in the proper sense of the word, but are largely due to superposed Fraunhofer lines.* The first impression which any observer would receive from an examination of exposures such as these is contained in the quoted description in the opening lines of the present paper, but there is little doubt that this is misleading. It is possible, indeed, that the chromosphere, defined as that part of the Sun near the limb which gives emission lines, has little continuous spectrum of its own. Fortunately the measures of paper II were made to be as far as possible independent of the "self-reversals" seen on the plate, whatever their origin, either by selecting lines weak in the Fraunhofer spectrum, or by measuring as high up in the chromosphere as the exposures would allow, and it is believed that the results published are unaffected by the change of view just now mentioned.

Another conclusion which can now be made is that the line profiles obtained by Thackeray† from the 1936 eclipse spectrograms are almost certainly not the true transition profiles, but the results of superposition of emission and absorption lines, coming in reality from adjacent parts of the solar image and mixed by the seeing, the various shapes observed being conditioned primarily by the strengths of the emission lines relative to their respective partners in absorption. The correction process used in the present work could not be applied to the 1936 spectra, which were photographed through the edge of a rapidly oncoming cloud, and in fairness to Dr. Thackeray it must be said that it was difficult to reach any other conclusion on the basis of the material available to him. Furthermore, it is unlikely that the 1940 observations would have been undertaken but for his work.

Although frustrated in our original purpose, we can nevertheless obtain some extremely valuable information, by comparing absorption line intensities just within the limb with those from the centre of the disk. Equivalent widths of 251 lines have been measured on the corrected spectrum from exposure 2. To decrease accidental errors 91 lines were also measured on the corrected spectrum from exposures 3 and 5, and since line intensities do not appear to have been changing extremely rapidly while these exposures were being taken, we have for these 91 lines used mean values from the two independent measures. Judging by the inter-agreement between pairs of equivalent widths of the same line, the average error of a single measure is about 17 per cent. Below equivalent width 0·020 A. the measures must be regarded as doubtful. Accidental errors for our purposes are not a very serious source of trouble; as is so often the case, the greatest dangers lie in systematic errors which cannot be revealed by examining internal consistency. One such error was encountered in the earlier work of measuring the profiles of the chromospheric emission lines and it will equally affect the work here.

* A footnote to this effect was sent for publication with the paper and received by the Society, but was subsequently lost as a result of enemy action.

† *M.N.*, 97, 672, 1937.

We recall that it arose from the fact that the plate was calibrated with an exposure time 30 seconds, while the spectra being measured had exposures about 0·6 second. A corrected calibration curve obtained during the course of the earlier work was therefore used for a re-reduction of a section of exposures 1 and 2, and it was found that the revised equivalent widths could be represented quite closely by a uniform increase of 10 per cent. in the original values. This correction then has been applied to the measures before being used in Fig. 4, where the limb equivalent widths are plotted against Allen's

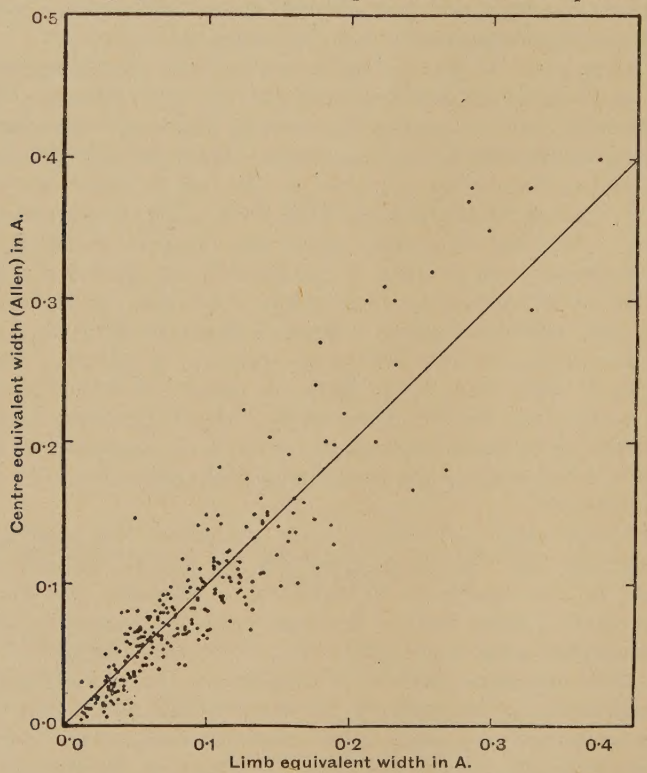

FIG. 4.—*Comparison of equivalent widths near the limb, at* $\cos\theta = 0{\cdot}05$, *with those measured by Allen at the centre of the disk. The diagonal line is for equality between centre and limb.*

equivalent widths for the centre of the disk. The figure shows that weak lines of equivalent width less than about 0·13 A. are as strong, or perhaps slightly stronger, at the limb than at the centre of the disk, while above this value there is a progressive weakening of the limb lines relative to centre lines, the difference increasing with line strength. It is at first sight surprising that the spectrum practically at the limb should be so nearly the same as that at the centre of the disk, and it must be admitted that there may possibly be undetected systematic errors in our work of the order of 10 per cent.; such errors are difficult enough to avoid in ordinary spectrophotometry of the Sun, when conditions are generally much more favourable for accuracy than at an eclipse. Nevertheless our measures are not inconsistent with those of Miss Adam*, who a few years ago discovered that weak Fraunhofer lines are actually strengthened at $\cos\theta = 0{\cdot}31$ in comparison with the centre of the disk, and it seems unlikely that the errors of the present work are so great as to vitiate the results seriously.

Theory.—The next task is to find, if possible, parameters in the standard Fraunhofer line theory which will give the observed behaviour of line depth as a function of θ. We

* *M.N.*, 98, 112, 1938; 100, 595, 1940.

start by using the method followed by Miss Adam, but now with the considerable advantage of having observations for a much smaller value of $\cos\theta$. The general procedure follows Eddington, using his well-known equation of transfer

$$\cos\theta\frac{d\mathcal{J}_\nu'(\theta)}{d\tau}-(1+\eta)\mathcal{J}_\nu'(\theta)+(1-\epsilon)\eta\mathcal{J}_\nu'+(1+\epsilon\eta)\mathcal{J}_T=0.$$

This is a monochromatic equation referring only to frequency ν. $\mathcal{J}_\nu'(\theta)d\nu$ is the flow of radiation of frequency ν to $\nu+d\nu$ within the spectrum line, in a direction making an angle θ with the outward normal to the solar surface, and $\mathcal{J}_\nu'=\frac{1}{4\pi}\int\mathcal{J}_\nu'(\theta)d\omega$, the integration being taken over a sphere. τ is optical depth in the continuous spectrum, measured perpendicular to the surface, $\mathcal{J}_T$ is the intensity of emission in the continuous spectrum, η is the ratio of line absorption coefficient to continuous absorption coefficient, and ϵ is the fraction of atoms de-excited by super-elastic collisions. First a solution for $\mathcal{J}_\nu'$ has to be found, using the well-known approximation

$$K_\nu'=\frac{1}{4\pi}\int\mathcal{J}_\nu'(\theta)\cos^2\theta\,d\omega=\tfrac{1}{3}\mathcal{J}_\nu',$$

and then, with the aid of this $\mathcal{J}_\nu'$, the equation of transfer is solved for $\mathcal{J}_\nu'(\theta)$, the quantities η, ϵ and $\mathcal{J}_T$ being given as functions of τ. The number of cases in which this can be done algebraically is very limited, and for most practical applications recourse must be had to numerical evaluation of particular examples.

$\mathcal{J}_T$ is given us by the observed darkening to the limb in the continuous spectrum.* Unfortunately, however, closely accordant results between different observers of limb darkening are not yet available, and no measures go as near the limb as is desirable, on account of formidable practical difficulties. Consequently there is still a fair amount of uncertainty in the numerical values of $\mathcal{J}_T$. It is frequently assumed that $\mathcal{J}_T$ is a linear function of τ, which makes the law of darkening a linear function of $\cos\theta$. This is a tolerably good first approximation, but a reference to Plaskett's paper, or to later work by Plaskett † and by Busbridge ‡, shows that it is not particularly accurate.

The parameters which can be varied are η and ϵ; indeed, one of our principal aims is to find out more as to their behaviour with τ. The depth of an absorption line depends chiefly on the integral of η with respect to τ, taken through the surface layers down to optical depth 1 or 2, but is rather insensitive to the way in which η is distributed through these layers, unless $\cos\theta$ is fairly small. Partly for this reason, but chiefly as a mathematical convenience, the assumption is frequently made that η is constant with respect to τ, although from a physical point of view this is not altogether satisfactory. The parameter ϵ can vary between the limiting values 0 (for pure scattering) and 1 (for pure absorption). Its value depends on the frequency of atomic collisions and may be supposed to approach zero in very high layers of the atmosphere and increase to unity when one descends to sufficiently great depths. Theorists are usually content to employ one or other of these two limiting values, $\epsilon=0$ being the more often used, and to apply it to all optical depths.

Although for the most part we have to work arithmetically, it is possible to demonstrate algebraically the unsuitability of one popular model atmosphere. If $\eta=$constant, $\epsilon=0$, and $\mathcal{J}_T=a+b\tau$, a and b being constants, with $b>a$, it is a straightforward matter to show that $\dfrac{dr}{d(\cos\theta)}$ is always negative, where r is the intensity within an absorption line, measured as a fraction of the adjacent continuous spectrum. Hence, proceeding from centre to limb, with $\cos\theta$ decreasing, r always increases and the line always weakens. This model, then, cannot be satisfactory for weak Fraunhofer lines. Apart from this

* H. H. Plaskett, *M.N.*, 96, 402, 1936. † *M.N.*, 101, 3, 1941. ‡ *Ibid.*, 26, 1941.

we have been obliged to proceed by arithmetical solution of special cases, a method which is not only tedious and laborious, but also does not give the insight into the problem which general algebraic solutions provide. Most of the computations have been made for λ 4100, one of Miss Adam's two wave-lengths, which for our purposes is sufficiently near the region over which the eclipse measures were made ($\lambda\lambda$ 4175–4560). Miss Adam, in Fig. 4 of her second paper, gives the $\mathcal{J}_T$ distribution for λ 4100, based on Plaskett's temperature distribution which he derived from the observed darkening to the limb. This may be represented by the following approximation:—

$$\begin{aligned} 0 < \tau < 0{\cdot}3 \quad & \mathcal{J}_T = \quad 1 + 2{\cdot}883\tau, \\ 0{\cdot}3 < \tau < 0{\cdot}6 \quad & \quad -2{\cdot}120 + 13{\cdot}283\tau, \\ 0{\cdot}6 < \tau < 1{\cdot}3 \quad & \quad 5{\cdot}85 \\ 1{\cdot}3 < \tau < \infty \quad & \quad 1{\cdot}59 + 3{\cdot}28\tau, \end{aligned}$$

which represents the given curve probably much more accurately than the latter itself has been determined. Using this, a considerable number of trials were made and the upshot was that no model in which there is pure scattering will give absorption lines at $\cos\theta = 0{\cdot}05$ of about the same strength as at $\cos\theta = 1$; it was necessary to have pure absorption, *i.e.* $\epsilon = 1$, right up to the surface $\tau = 0$. One of the more promising examples was

$$\left.\begin{aligned} 0 < \tau < 0{\cdot}05 \quad & \eta = 0{\cdot}59 \\ 0{\cdot}05 < \tau < 0{\cdot}3 \quad & \quad 0{\cdot}22 \\ 0{\cdot}3 < \tau < 0{\cdot}6 \quad & \quad 0{\cdot}075 \\ 0{\cdot}6 < \tau < 1{\cdot}3 \quad & \quad 0{\cdot}0 \\ 1{\cdot}3 < \tau < \infty \quad & \quad 0{\cdot}0 \end{aligned}\right\} \begin{aligned} &\epsilon = 1 \\ &\mathcal{J}_T \text{ as above,} \end{aligned}$$

which gives

$\cos\theta = 1{\cdot}00$	(centre of disk)	$r = 0{\cdot}931$
$0{\cdot}31$	(Miss Adam's observations)	$0{\cdot}870$
$0{\cdot}05$	(eclipse observations)	$0{\cdot}957$.

Here there is a strengthening of weak lines between $\cos\theta = 1{\cdot}00$ and $0{\cdot}31$, while an absorption line is produced at $\cos\theta = 0{\cdot}05$, of the same order of strength as at the centre. This result is hopeful, but closer examination forces us to reject it. We know little of the true shapes of the fainter Fraunhofer lines under consideration, but can be certain that their true central intensities are lower than what we observe, on account of instrumental distortion. Now lines whose observed central intensities are about $0{\cdot}5$ are found to have approximately the same equivalent width at $\cos\theta = 0{\cdot}05$ as at the centre of the disk. Admitting that our observations do not permit too much certainty on this point, it nevertheless seems necessary to find a model which will predict no very great weakening between $\cos\theta = 1$ and $\cos\theta = 0{\cdot}05$ for $r = 0{\cdot}5$, or which will at least permit r to be as low as $0{\cdot}5$ at $\cos\theta = 0{\cdot}05$, whatever the corresponding value at $\cos\theta = 1$ may be. This the above model will not do. For example, if η is multiplied by 10 everywhere, we get

$\cos\theta = 1{\cdot}00$	$r = 0{\cdot}533$
$0{\cdot}31$	$0{\cdot}480$
$0{\cdot}05$	$0{\cdot}891$.

In the case of pure absorption, the minimum intensity possible within any Fraunhofer line, however strong, is the intensity $\mathcal{J}_T$ for $\tau = 0$. The blackest possible line has a central intensity which remains constant across the disk, if measured absolutely. But if referred to the adjacent continuous spectrum, which as one proceeds to the limb also tends to the value which $\mathcal{J}_T$ has at $\tau = 0$, the minimum intensity increases with decreasing $\cos\theta$, reaching unity at the limb. All lines vanish at the limb, while at $\cos\theta = 0{\cdot}05$ strong lines have proceeded proportionately much farther towards disappearance than have weak lines. It happens that this is in qualitative agreement with our observations, but

quantitatively there is a wide discrepancy between observation and the theoretical model, and no reasonable amount of observational error is sufficient to bridge the gap.

When $\epsilon = 1$, the computed line depths near the limb, particularly for the rather extreme case $\cos\theta = 0{\cdot}05$, are highly sensitive to changes in $\mathcal{J}_T$ for small τ. If we examine the $\mathcal{J}_T$ values with which we have been working we find that the first observed point on Plaskett's curve is for $\tau = 0{\cdot}1$, and that what has been used for $0{\cdot}0 < \tau < 0{\cdot}1$, a region now of critical importance, is really an extrapolation. It is highly tempting to suppose that there is in fact some rounding off of the curve very near $\tau = 0$, which will reduce $\mathcal{J}_T$ at the surface considerably below the value used so far. Indeed Miss Busbridge's work shows that it is possible to modify $\mathcal{J}_T$ in this manner and still satisfy the limb-darkening observations. This solution is, however, not permissible. There is a well-known relation between the effective temperature and surface temperature of a star, which elementary theory gives as $T_e^4 = 2T_0^4$, or more exact theory as

$$T_e^4 = \frac{4}{\sqrt{3}} T_0^4 = 2{\cdot}309 T_0^4.*$$

This is based on such general considerations that it is extremely difficult to see how it can be evaded, and it gives a $\mathcal{J}_T$ for $\tau = 0$ not far from Plaskett's curve, so that no considerable deviation from this can be allowed in the region very near the surface.

Failing the discovery of a mechanism for reducing $\mathcal{J}_T$ near the surface, or for transferring the energy to other regions of the continuous spectrum and so effectively reducing it, *there appears to be no combination of parameters in ordinary Fraunhofer line theory which will explain the observations at* $\cos\theta = 0{\cdot}05$. We thus have to think of some physical agency known to be present on the surface of the Sun and not included in the theory. We naturally turn to the non-uniformity of the surface, and in particular to the rice-grain structure, the solar granulation, which is a permanent and characteristic feature of the Sun. The granules, so far as present knowledge goes, are irregular patches of the order of 10 per cent. brighter than their surroundings, their average diameter is about 3500 km. and their average separation about twice this, say 7000 km. (We note that these dimensions are large compared with the thickness of the layers which give us the Fraunhofer spectrum.) They are in a state of continuous change, the average lifetime of an individual granule being about 3 minutes.† They can be observed all over the solar disk and at all phases of the sunspot cycle. Plaskett considers them to be caused by warmer matter brought up from below by some form of turbulence, and in any case it seems natural to suppose that they are associated with vertical movement of matter, although the actual velocities are still a matter for debate. Velocities up to 4 km./sec. have been reported by Hansky and Chevalier, but Evershed ‡ more recently was unable to find velocities more than about 0·2 km./sec., and that not at the centre of the disk. However, direct observations of velocities in the individual granules are extremely difficult to make, and indirect evidence from the shapes of the Fraunhofer lines may be more reliable. In the conditions under which spectrograms are usually obtained for the measurement of line profiles, the spectrograph slit receives light from an appreciable area of the disk, probably covering a fair number of granules. Now line profiles measured by Allen § were found by him to be consistent with a "large scale turbulence" with a most probable (vertical) velocity of 1·8 km./sec., and a rather similar conclusion was later reached by ten Bruggencate || from independent observations. At about the same time as Allen's work, the present writer ¶ on the basis of still other evidence, namely the central intensities of a few very strong Fraunhofer lines, suggested a similar form of motion, with a velocity of 1 to 1·5 km./sec. We may tentatively connect these velocities with the

* Unsöld, *Physik der Sternatmosphären*, 103, 1938.
† Plaskett, *M.N.*, 96, 402, 1936; ten Bruggencate and Grotrian, *Z. f. Ap.*, 12, 323, 1936.
‡ *M.N.*, 94, 96, 1933.
§ *Ap. J.*, 85, 165, 1937.
|| *Z. f. Ap.*, 18, 316, 1939.
¶ *M.N.*, 97, 552, 1937.

granules on the surface, although the association so far lacks definite demonstration, and picture the granules as rising and falling with respect to the mean surface of the Sun, probably in some fairly regular phase relationship with their changes of surface brightness.

Although our knowledge is far less precise than could be desired, it appears reasonable to suppose that the granules cause a geometrical irregularity in the solar atmosphere, that the surface in fact is bumpy. The average wave-length of the irregularities will be taken to be 7000 km., following the evidence mentioned above, and the average semi-amplitude 350 km. (2 km./sec. for 3 minutes is 360 km.). A full discussion of the effect of this surface roughness on Fraunhofer line theory is impossible at the moment, and a rather crude treatment must suffice here. We shall suppose that every element of surface radiates just as it would if forming part of the static, level atmosphere postulated by the usual theory. This assumption is not in strict accordance with the facts, for it ignores the surface brightness changes by which the granules are detected, but in its favour can be adduced the large horizontal scale of the granules compared with the thickness of the atmospheric layers with which we are concerned, and the relatively small height of the "bumps." On the other hand, the curvature of the "bumps" is much greater than that of the Sun's smooth surface, so that when θ is near 90° their optical thickness in the line of sight may be insufficient for standard theory to be applicable.* We shall suppose, however, that the effect on the spectrum arises solely from the change in θ. This angle is no longer given simply by position on the Sun's disk, but its mean value has to be computed from the assumed average shape of the surface irregularities. In the simplest possible case the surface was taken to consist of one-dimensional waves of the form

$$z = 0{\cdot}05 \sin 2\pi x,$$

the axes of x and y being in the plane of the undisturbed surface, and of z along the outward normal, while the unit of z is one wave-length. Our eclipse observations were made at apparent $\theta = 87°$, *i.e.* apparent $\cos\theta = 0{\cdot}05$, so that the direction cosines of the line of sight were

$$(\sin 87° \cos\alpha, \quad \sin 87° \sin\alpha, \quad \cos 87°).$$

If the surface contains a large number of waves with arbitrary orientations, α must be regarded as being able to take all values between 0° and 90°.

The angle θ' between the normal to the surface and the line of sight is given by

$$\cos\theta' = \frac{1}{\sqrt{(1 + 0{\cdot}01\pi^2 \cos^2 2\pi x)}}[-0{\cdot}1\pi \cos 2\pi x \sin 87° \cos\alpha + \cos 87°].$$

The line of sight is tangential to the surface at (x_1, y_1, z_1), where

$$0{\cdot}1\pi \cos 2\pi x_1 = \cot 87° \sec\alpha$$

and meets the surface again at (x_2, y_2, z_2), where

$$0{\cdot}05(\sin 2\pi x_2 - \sin 2\pi x_1) \sin 87° \cos\alpha = (x_2 - x_1) \cos 87°$$

and the visible part of the surface lies between x_1 and x_2.

In evaluating the mean value $\bar{\theta}$, we have to take into account the fore-shortening of any element of surface, and also the darkening to the limb, now more correctly described as the variation of surface brightness with θ. For this we have adopted the values corresponding to the $\mathcal{J}_T$ used above, although it is clear that the darkening to the limb observations ought also to be rediscussed, taking into account the roughness of the surface.

* *Cf.* Woolley, *M.N.*, 98, 3, 1937. Were the surface perfectly smooth, one would have to go considerably nearer the limb than $\cos\theta = 0{\cdot}05$ before the optical thickness in the line of sight becomes small enough for Woolley's work to apply.

Then

$$\bar{\theta} = \frac{\int_{x_1}^{x_2} \theta' \cdot \cos\theta' \cdot \mathcal{J}_\nu(\theta') \cdot dl}{\int_{x_1}^{x_2} \cos\theta' \cdot \mathcal{J}_\nu(\theta') \cdot dl}$$

where $\mathcal{J}_\nu(\theta')$ is the surface brightness for θ', calculated from the adopted $\mathcal{J}_T$, and

$$dl = \sqrt{(1 + 0{\cdot}01\pi^2 \cos^2 2\pi x)}dx$$

is an element of length along the wave profile. We calculate $\bar{\theta}$ for a representative series of values of α and then average over all α. The result is

$$\bar{\theta} = 78°{\cdot}4, \qquad \cos\bar{\theta} = 0{\cdot}20,$$

whereas the apparent values were 87° and 0·05 respectively. If we start with apparent $\theta = 72°{\cdot}5$, apparent $\cos\theta = 0{\cdot}3$, corresponding to Miss Adam's observations, we find $\bar{\theta} = 67°{\cdot}1$, $\cos\bar{\theta} = 0{\cdot}39$. The change here is less important, although still not negligible.

The slightly more complicated case where the surface consists of large numbers of two-dimensional "waves" of the form

$$z = 0{\cdot}05 \cos 2\pi\sqrt{x^2+y^2} = 0{\cdot}05 \cos 2\pi r, \qquad 0 \leqslant r \leqslant \tfrac{1}{2}$$

has also been worked out. It gave a result very close to the above, namely for apparent $\theta = 87°$, apparent $\cos\theta = 0{\cdot}05$, the effective $\bar{\theta} = 76°{\cdot}8$ and $\cos\bar{\theta} = 0{\cdot}23$. In this case the screening of one wave by others was neglected.

It is useless at the moment to try to make any estimate more precise than this, so much depends on the wave shape, and more especially on the amplitude relative to the wave-length. Besides, the granulation phenomenon is essentially irregular, as may be seen on any good photograph*, and can be represented only very artificially by simple formulæ of the kind we have been considering. There is thus a good deal of latitude in quantitative results. We have probably a little overestimated the amplitude in the vertical co-ordinate, but it appears that a roughness of the Sun's surface of a kind consistent with granulation and line-profile observations may convert an apparent $\cos\theta = 0{\cdot}05$ to an effective $\cos\bar{\theta}$ about 0·20. This result might have been predicted quite independently of our eclipse results; that it also provides a way to explain the observed Fraunhofer spectrum extremely near the limb encourages the belief that an effect of this kind is actually operative on the Sun. It gives also another reason why the polarization in Fraunhofer lines near the limb is found to be much less than the theoretical value predicted by Zanstra.†

We shall as a first approximation regard the correction to the apparent θ as being the same for both continuous spectrum and for points within Fraunhofer lines. This is not strictly true and tends to exaggerate the effect of the roughness of the surface in the case of the weaker lines. It is, however, sufficient for a first guide and later we shall give an example of the more accurate method, involving considerably more computation, for which

$$\bar{r} = \frac{\int \mathcal{J}_\nu'(\theta') \cos\theta' dl}{\int \mathcal{J}_\nu(\theta') \cos\theta' dl}$$

where $\mathcal{J}_\nu'(\theta')$ is the intensity within the line at the surface of the atmosphere, $\mathcal{J}_\nu(\theta')$ is the corresponding intensity in the continuous spectrum, and each integral is taken over the whole wave surface.

The task of reconciling Fraunhofer line theory with the eclipse observations and

* *E.g.* ten Bruggencate and Grotrian, *Z. f. Ap.*, 12, 328, 1936.

† *M.N.*, 101, 250, 273, 1941.

with the observations of Miss Adam may now be resumed with more hope of success. At the same time it is desirable to take into consideration the measures of strong lines recently published by Houtgast.* There is no intention of making here an exhaustive discussion of the whole centre-limb problem for all Fraunhofer lines, but it is obviously undesirable to suggest a model atmosphere for weak lines which has no hope of ever giving satisfactory results for strong lines. If we are to have a theory in which centre-limb behaviour depends solely on r, the wings of strong lines should show some strengthening between $\cos\theta = 1{\cdot}0$ and $0{\cdot}3$ (apparent values) to agree with Miss Adam's results for weak lines. According to Houtgast's measures, not all lines show this effect. It appears to be absent in the case of the H and K lines and also the infra-red triplet of

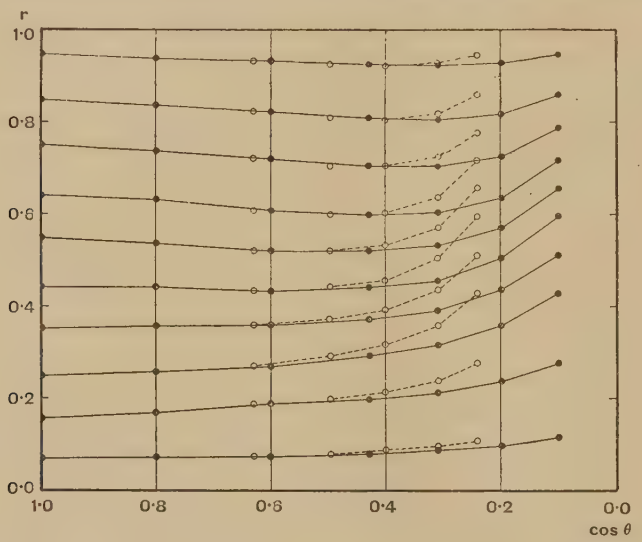

FIG. 5.—*Variation of r with cos θ for strong lines of FeI and CaI, according to Houtgast's measures. Unfilled circles and dotted lines show the effect of correcting θ as explained in the text.*

*Ca*II; it is weak in the case of the *Mg*I *b* lines, the *Mg*I λ 3830 triplet, and the *Na*I D lines; in the rest of his lines, namely *Fe*I λλ 3815·9, 3820·4, 3859·9, 4005·3, 4045·8, 4063·6, 4071·8, 4143·9, and *Ca*I λ 4226·7, the strengthening is, however, quite well marked. We see that a complete theory will have to study each line individually. For the present we shall restrict our attention to the *Fe*I and *Ca*I lines, whose behaviour appears to be consistent with Miss Adam's work on weak lines. Mean curves obtained by averaging all Houtgast's measures for these lines, after grouping according to r at the centre of the disk, $0 < r < 0{\cdot}1$, $0{\cdot}1 < r < 0{\cdot}2$, etc., are given in Fig. 5, with dotted curves to show the effect of correcting the apparent θ by the method used above (one-dimensional case). When examining the values for $\cos\theta = 0{\cdot}1$, and to some extent those for $\cos\theta = 0{\cdot}2$, the reader should remember the considerable practical difficulty, pointed out by Houtgast, of observing in full daylight so near the limb, where there is much danger of contamination by light from adjacent parts of the disk, on account of scintillation and scattering. Nor should it be forgotten that it is impracticable to correct full daylight observations for chromospheric light coming from just outside the disk.

There appear to be at least two model atmospheres which will give a deepening of Fraunhofer lines between $\cos\theta = 1$ and $\cos\theta = 0{\cdot}4$, for $0{\cdot}5 < r < 1{\cdot}0$, namely (*a*) an

* "The Variations in the Profiles of Strong Fraunhofer Lines along a Radius of the Solar Disk," Dissertation, Utrecht, 1942. I am indebted to Dr. Zanstra for the good fortune of being able, despite present circumstances, to examine a copy of this.

atmosphere with pure absorption, $\epsilon = 1$, with η decreasing with optical depth, and (*b*) an atmosphere with pure scattering, $\epsilon = 0$, with the formation of the absorption line taking place either above $\tau = 0$, or at extremely shallow optical depths. This is essentially the well-known Schuster-Schwarzschild model. In both cases the line strengthening is dependent on the values of $\mathcal{J}_T$ which are used. To illustrate this, computations have been made both with the $\mathcal{J}_T$ for λ 4100 derived from Plaskett's work and already used, and with a linear $\mathcal{J}_T = 1 + 4\tau$, corresponding to a darkening to the limb law $\mathcal{J} = \mathcal{J}_0(\frac{1}{5} + \frac{4}{5}\cos\theta)$, which is approximately true for this region.

For the pure absorption model we have used

$0 < \tau < 0{\cdot}3$	$\mathcal{J}_T =$ $1 + 2{\cdot}883\tau$	$\eta =$ ξ	$\epsilon = 1$
$0{\cdot}3 < \tau < 0{\cdot}6$	$-2{\cdot}120 + 13{\cdot}283\tau$	ξ	
$0{\cdot}6 < \tau < 1{\cdot}3$	$5{\cdot}85$	$0{\cdot}3\xi$	
$1{\cdot}3 < \tau < \infty$	$1{\cdot}59 + 3{\cdot}28\tau$	$0{\cdot}1\xi$	

and the curves giving r as a function of $\cos\theta$ are in Fig. 6. The deepening of the line between $\cos\theta = 1$ and 0·4 may be made greater by increasing the rate at which η falls

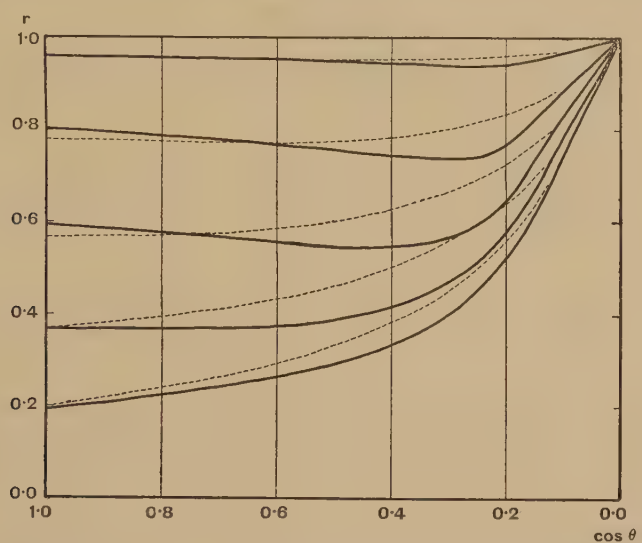

FIG. 6.—*Variation of r with cos θ in a pure absorption model. The continuous curves were computed with Plaskett's $\mathcal{J}_T$; the dotted curves with a linear $\mathcal{J}_T$. The lowest curve in each case gives the minimum r.*

off with increasing τ. With η constant with respect to τ the curves become very much flatter, the decrease from $\cos\theta = 1$ to 0·4 being of the order of one-quarter of that shown, when r is near 0·75. The decrease is also very much reduced if the linear $\mathcal{J}_T$ is used, η remaining as above. It is clear that no close quantitative study of curves such as these can be made until more accurate data for $\mathcal{J}_T$ are available. Taking the Plaskett $\mathcal{J}_T$ as the more reliable, we can say that this model is satisfactory for weak lines, but quite unsuitable for strong lines, as r can never fall below the lowest curve in the figure, contrary to observation.

For the pure scattering model (*b*) we have used the same $\mathcal{J}_T$ as above to give the continuous spectrum of the photosphere. The quantity $H_\nu' = \frac{1}{4\pi}\int \mathcal{J}_\nu'(\theta)\cos\theta\, dw$ is constant throughout the scattering atmosphere and its value is found by direct integration at $\tau = 0$, in the same manner as is followed in deducing the standard Schuster-Schwarzschild

formula (Milne). If s_1 is the total optical depth *in the absorption line* of the scattering atmosphere

$$\underset{\text{surface}}{\mathcal{J}_\nu'(\theta)} = H_\nu'(2+3\cos\theta) + e^{-s_1\sec\theta}\left\{\underset{\tau=0}{\mathcal{J}_\nu'(\theta)} - H_\nu'(2+3s_1+3\cos\theta)\right\}.$$

If we use a linear $\mathcal{J}_T$, *i.e.* a cosine law of darkening to the limb, the results are exactly those of the Milne formula. The curves for r against cos θ are in Fig. 7. We note that again there is some strengthening of the line with diminishing cos θ, and that the course of the curves is dependent on $\mathcal{J}_T$. There is a general resemblance between these curves

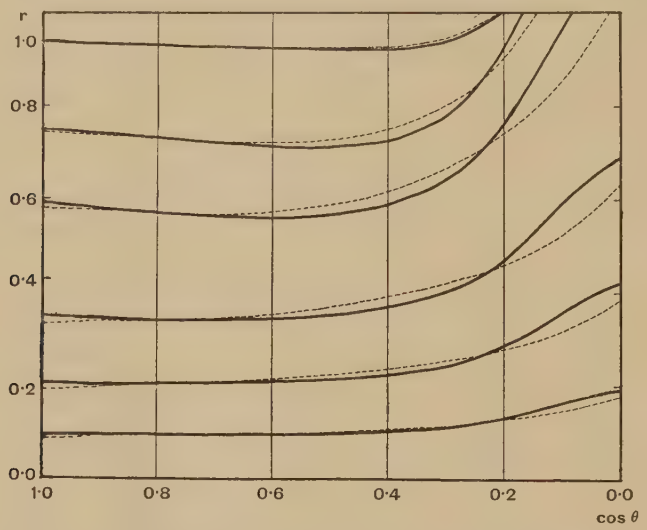

FIG. 7.—*Variation of r with cos θ in the Schuster-Schwarzschild model. From top to bottom the curves are for $s_1 = 0{\cdot}1$, 0·5, 1·0, 2·5, 5·0 and 12·5 respectively. Continuous curves were computed with the Plaskett $\mathcal{J}_T$; dotted curves with a linear $\mathcal{J}_T$.*

and those given by Houtgast's observations. The model is satisfactory for r below 0·5, but unsatisfactory above this, for turning to our eclipse observations, which are unlikely to refer to an effective cos θ greater than 0·2, we see that the model predicts that here the weakest lines will already have turned into emission, while there is a considerable weakening for all lines whose r at the centre of the disk is greater than about 0·6, contrary to what we have observed.

In many ways these two models are complementary; where one succeeds the other fails, and *vice versa*, which suggests that the two be combined into what may be termed a modified Schuster-Schwarzschild model, in which the photosphere of the standard S-S model is replaced by layers in which the Fraunhofer line is being formed by pure absorption, so that before the light has entered the base of the scattering atmosphere the line is already in existence. The pure scattering atmosphere lies wholly above $\tau = 0$ and is taken to be comparatively thin. Computations have been made with the following:

Above $\tau = 0$, pure scattering, $\epsilon = 0$, with $s_1 = 0{\cdot}05\xi$.
Below $\tau = 0$, pure absorption, $\epsilon = 1$, with η and $\mathcal{J}_T$ as in model (*a*).

Since the properties of the pure absorption layers are determined solely by the assumed distribution of η and by the distribution of $\mathcal{J}_T$, which is supposed to be given by the observed darkening to the limb, they are for computational purposes independent of the scattering atmosphere above. We integrate for H_ν' at $\tau = 0$, and evaluate $\mathcal{J}_\nu'(\theta)$ at the surface very much as before.

The curves for r are shown in Fig. 8. We now get weak lines at cos $\theta = 0{\cdot}2$ slightly

stronger than at the centre of the disc (eclipse observations); we have strengthening of weak lines between cos $\theta = 1$ and 0·4 (Miss Adam's observations); and we have curves which bear a general resemblance to those from Houtgast's observations for all r in strong lines of *Fe*I and *Ca*I. In connection with the latter we remind the reader once more of the observational difficulties for small cos θ, and the fact that we do not know definitely the correction from apparent to effective θ very near the limb. The computed curves are for λ 4100, but calculations for λ 5100 show similar results.

If we follow the more accurate procedure, mentioned above, of computing the

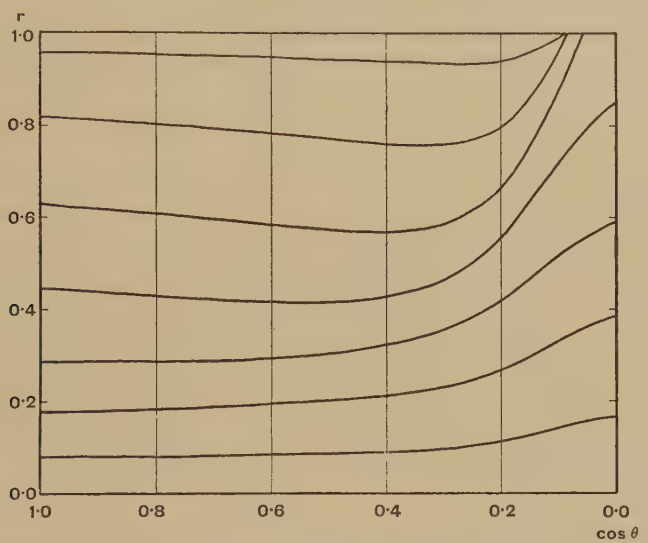

Fig. 8.—*Variation of r with cos θ for a modified Schuster-Schwarzschild model. From top to bottom the curves are for* $\xi = 0{\cdot}1$, 0·5, 1·25, 2·5, 5·0, 12·5 *and* 62·5 *respectively.*

effective $\bar{r}$ at cos $\theta = 0{\cdot}05$, instead of using a correction to θ the same both within and without the absorption line, we get the following results for the model last mentioned:

cos $\theta = 0{\cdot}05$	cos $\theta = 0{\cdot}05$
$r = 0{\cdot}959$	$\bar{r} = 0{\cdot}954$
·817	·832
·628	·695
·445	·562
·287	·419
·176	·270
·079	·115

For strong lines it is very much the same whether we use this method or the other; for weak lines the "effective θ" method exaggerates the consequences of the surface roughness. However, in either case the agreement between theory and observation is now as close as we can expect.

The model now under discussion cannot be claimed to be unique, in the sense that no other will give agreement with observation. It is a natural elaboration of the S-S model, and the latter, in relation to its simplicity, has generally been regarded as very successful. In the present case we have in effect divided the outer layers of the Sun into two parts: an upper in which atomic collisions are unimportant, where therefore little continuous spectrum is produced and light coming from below is subjected only to scattering; and a lower in which collisions are dominant, where continuous spectrum is produced and excited atoms lose their energy chiefly in collisions. This may be a drastic over-simplification, but a theoretical model must be judged by its results and

cannot be expected to represent the complexities of the actual state of affairs in full detail. The assumption that η decreases with depth in the pure absorption layers is what is generally anticipated, owing to the increase of the continuous absorption coefficient with τ, although it is only fair to say that Plaskett * recently derived an η *increasing* rapidly with τ for the *Mg* b lines. The course of r with θ can be modified to a certain extent by changing the gradient of η with respect to τ. We can also alter the thickness of the scattering layer according to whether we wish to approach more nearly the pure absorption case on the one hand, or the regular S-S model on the other. The greatest weakness at the moment lies in the uncertainty in $\mathcal{J}_T$ as a function of τ, and in our ignorance as to the effect of the roughness of the Sun's surface on centre-limb changes. These affect all studies of centre-limb behaviour of Fraunhofer lines, not merely the present investigation alone, and for the time being constitute the principal barriers to further progress. Until more definite knowledge is available on these points, a close quantitative comparison of any theory with observation is premature.

Houtgast in his dissertation maintains that it is necessary to take into account non-coherent scattering before his observations can be satisfied. That such a process is physically possible, or even probable, cannot be denied. That this, or any other mechanism involving the introduction of an additional parameter into the theory, makes it in general easier to get agreement with observation is also incontestable. The theory with coherent scattering, however, permits such a wide range of models, and so few of the available mathematical combinations can as yet be rejected on physical grounds, that the present writer remains unconvinced that we are at the moment compelled by the *astronomical* evidence alone to take non-coherent scattering into account. The issues raised are in any case too complicated to be dealt with in this paper, which is primarily concerned with matters arising directly out of the 1940 eclipse observations.

The writer wishes to record his thanks to Dr. H. Zanstra for much valuable criticism.

Radcliffe Observatory,
Pretoria:
1943 *April.*

* *M.N.*, 101, 3, 1941.

NOTE ON CONVECTION IN THE SUN

R. v. d. R. Woolley

(Received 1943 May 14)

Summary

A new relation is put forward between the mean life, contrast and size of the granulation. Observed values of these three quantities indicate a velocity between 2 and 3 km./sec. for convection movements. The temperature gradient is little disturbed from the Milne value.

---

1. In an important paper * Sir Arthur Eddington discussed convection in the outer layers of the Sun and raised an important question about ionization equilibrium which was satisfactorily answered by Schwarzschild †, whose views Eddington accepts. ‡ We may once again suppose that when a mass of gas moves convectively in the outer parts of the Sun the ionization will be given by Saha's relation, using a temperature defined by the thermal motion of the particles. In the present note the writer's previous paper on convection § (which assumed Saha ionization) is modified, and a new relation between the contrast, mean life and size of the granulation is brought forward.

The notation is that of the writer's previous paper. Let T_1, ρ_1, ξ_1 be the temperature, density and velocity of upward-moving matter and let the upward-moving matter occupy the fraction α_1 of the Sun's surface; and let T_2, ρ_2, ξ_2, α_2 be the corresponding quantities for downward-moving matter. If all the matter is moving up or down then $\alpha_1+\alpha_2=1$. Define a mean temperature T by $T^4=\alpha_1 T_1^4+\alpha_2 T_2^4$ and let $T_1=T(1+\alpha_2\gamma)$. Then if γ is small, $T_2=T(1-\alpha_1\gamma)$. Now the net flux of energy in the outer layers of the Sun is constant, part being carried by radiation and part by convection. This leads to the equation

$$T_0^4=\tfrac{8}{3}T^3\frac{dT}{d\tau}+\frac{2\alpha_1\rho_1\xi_1}{ac}C_p\gamma T, \tag{1.1}$$

where C_p is the specific heat at constant pressure. This equation is developed in detail in *M.N.*, **101**, 55–57, 1941.

Again, let K be the kinetic energy of one gramme of the gas and E its internal energy. Let one gramme of the gas pass from state 1 to state 2 doing work W_{12} and losing to its surroundings the quantity of heat Q_{12}. Then from the conservation of energy,

$$K_1+E_1=K_2+E_2+W_{12}+Q_{12}.$$

If the gas moves along the x-axis with a velocity ξ, and if the heat loss is q ergs per gramme per second, we have

$$\frac{dE}{dx}+\frac{dW}{dx}+\xi\frac{d\xi}{dx}+\frac{q}{\xi}=0.$$

Let $\left(\frac{\partial(E+W)}{\partial T}\right)_p=L$ and $\left(\frac{\partial(E+W)}{\partial p}\right)_T=M$, and let $d\tau=-k\rho dx$. Then

$$\xi\rho\left\{L\frac{dT}{d\tau}+M\frac{dp}{d\tau}+\xi\frac{d\xi}{d\tau}\right\}=\frac{q}{k}. \tag{1.2}$$

---

* *M.N.*, 101, 177, 1941.
‡ *M.N.*, 102, 154, 1942.
† *M.N.*, 102, 152, 1942.
§ *M.N.*, 101, 52, 1941.

If q is zero and $\frac{d\xi}{d\tau}$ vanishes, then $\frac{dT}{d\tau}$ takes the adiabatic value $\left(\frac{dT}{d\tau}\right)_s$.

(For details see *M.N.*, **101**, 59, 1941, where explicit expressions for L and M are given.)

2. The heat loss q demands investigation from two points of view, firstly the amount of heat that can be transferred by a mass of gas which has adjusted its internal temperature distribution so as to get rid of heat, and secondly the time taken to adjust the internal temperature. We shall first suppose that the heat loss in an ascending granule is due to radiation alone and that there is no internal convection. We shall suppose that the unit is a sphere of radius a and that it is in radiative equilibrium. Let $I(\theta)\, d\omega/4\pi$ be the flow per sq. cm. per sec. of radiation travelling in directions within an infinitesimal solid angle $d\omega$ at an inclination θ to the radius vector, and let

$$\mathcal{J} = \frac{1}{4\pi}\int I(\theta) d\omega, \qquad H = \frac{1}{4\pi}\int I(\theta) \cos\theta d\omega.$$

Then the (approximate) equation of radiative equilibrium is

$$d\mathcal{J}/d\tau = 3H \tag{2.1}$$

(see Eddington, *Internal Constitution of the Stars*, pp. 101 and 322).

First consider the heat flow in a sphere in which there is no secular change of temperature but in which heat is created at the rate h ergs per sec. per unit volume. The amount of energy crossing a surface of radius r is $4\pi r^2 H$ ergs per second, and the difference between this amount and the amount crossing a surface of radius $r+dr$ is $4\pi d(r^2H)$. This difference is equal to the amount of heat created between radii r and $r+dr$, so that

$$4\pi d(r^2H) = 4\pi h r^2 dr.$$

Solving this equation subject to the condition $H=0$ at $r=0$ (no flux at the centre), we get

$$3H = hr.$$

Then from (2.1)

$$d\mathcal{J} = 3H d\tau = -k\rho h r dr.$$

Suppose that k and ρ are independent of r. Then

$$\mathcal{J} = \text{const.} - \tfrac{1}{2} k\rho h r^2.$$

Let H_0 be the flux at the outer boundary of the sphere $r=a$ and let $k\rho a = \tau_0$. Then

$$\mathcal{J} = \text{const.} - \frac{3}{2}\frac{r^2}{a^2} H_0 \tau_0. \tag{2.2}$$

Let T_1, T_0 be the temperatures of the centre of the sphere and of its outer boundary respectively. In radiative equilibrium $\mathcal{J} = \sigma T^4$. Let $H_0 = \lambda\sigma T_0^4$. Then (2.2) becomes

$$T^4 = T_1^4 - \frac{3}{2}\frac{r^2}{a^2}\tau_0 \lambda T_0^4.$$

This gives the temperature at any point in the sphere. In particular

$$T_1^4 = T_0^4(1 + \tfrac{3}{2}\lambda\tau_0),$$

and if $\lambda\tau_0$ is small compared with unity,

$$T_1 = T_0(1 + \tfrac{3}{8}\lambda\tau_0).$$

The mean temperature $\bar{T}$ is given by

$$\bar{T} = T_0(1 + \tfrac{3}{20}\lambda\tau_0),$$

and an effective temperature T_e (assuming τ_0 large compared with unity) is

$$T_e = T_0(1 + \tfrac{3}{8}\lambda).$$

Now suppose that the sphere is surrounded by material of mean temperature $\bar{T}' = \bar{T}(1 - \gamma)$, surface temperature $T_0' = \bar{T}'(1 + \frac{3}{2}\lambda\tau_0)$ and effective temperature $T_e' = T_0'(1 - \frac{3}{8}\lambda)$. Then $H_0 = \sigma T_e^4 - \sigma T_e'^4$, which gives

$$\lambda\tau_0 = \tfrac{10}{3}\gamma.$$

The heat loss from the whole sphere to its surroundings is $4\pi a^2 H_0$, so that the heat loss per gramme is $q = 3H_0/a\rho$. In terms of the mean temperature $\bar{T}$ this is

$$q = \frac{10\sigma\bar{T}^4}{a\rho\tau_0}(1 - 2\gamma). \tag{2.3}$$

Having established the rate of loss of heat in a steady state, the question arises, How long will the gas require to adjust its temperature distribution to give this heat loss? With no creation of heat the equation of flow of radiation is

$$d(r^2H) = -r^2 dr C\rho \frac{\partial T}{\partial t},$$

where C is the specific heat. This equation is

$$\frac{\partial}{\partial r}\left(r^2 \frac{3}{k\rho}\frac{\partial \mathcal{J}}{\partial r}\right) = r^2 C\rho \frac{\partial T}{\partial t},$$

or, since $\mathcal{J} = B$ in radiative equilibrium,

$$\frac{1}{r^2}\frac{\partial}{\partial r}\left(r^2 \frac{\partial B}{\partial r}\right) = \tfrac{1}{3}Ck\rho^2 \frac{T}{4B}\frac{\partial B}{\partial t}.$$

If we take a mean value of T/B and write $\frac{1}{3}Ck\rho^2 T/4B = \frac{1}{\kappa}$, the equation becomes

$$\frac{\kappa}{r^2}\frac{\partial}{\partial r}\left(r^2 \frac{\partial B}{\partial r}\right) = \frac{\partial B}{\partial t},$$

which is a well-known equation in the conduction of heat. Write $U = rB$. Then

$$\kappa \frac{\partial^2 U}{\partial r^2} = \frac{\partial U}{\partial t},$$

with the boundary conditions $U = 0$ at $r = 0$ and $U = U_1$ at $r = a$. The solution is

$$U = \sum b_m e^{-\kappa\left(\frac{m\pi}{a}\right)^2 t} \sin\frac{m\pi r}{a}.$$

The term which takes longest to die away is the first or $m = 1$. This term is reduced to $1/e$ of its value in $t_0 = a^2/\pi^2\kappa$ seconds. Now C is of order 10^9, k of order 100 and ρ of order 10^{-8}, so that with $T = 10^4$ and $a = 5 \times 10^7$ we find that κ is of order 10^{14} and t_0 of order 1 second. This is small compared with the duration of the convection process (of order 100 seconds), so that we may suppose that a sphere moving convectively will adjust its internal temperature gradient so as to radiate very nearly at the rate given by (2.3).

3. We now have to inquire whether a sphere moving upwards in the solar atmosphere would move as a whole or whether it would be subject to convection currents, and if so on what scale. Since the sphere is in the convection zone the ratio of its specific heats is less than 4/3, and the ordinary (vertical) temperature gradient of the solar atmosphere will not prevent convection currents within the sphere: the only question is whether

they will take place on a large enough scale to increase the heat transfer substantially above the radiative value (2.3). Now if there is no convection, the temperature at the centre of the sphere and at the boundary are related by the equation

$$T_1 = T_0(1 + \tfrac{5}{4}\gamma),$$

and the temperature difference between centre and boundary is $\frac{5}{4}T_0\gamma$, which is rather larger than the temperature difference between the upward and downward streams (which is $\bar{T}\gamma$). The internal velocities must accordingly be of the same order of magnitude as the velocity in the main movement, namely 2 to 3 km. per sec. Within a lifetime of 200 seconds there is just time for a sphere of radius 100 km. to *turn itself inside out*. The most rapid movement takes place in the centre: when material in the central column reaches the front of the movement it spreads itself out over the surface of the sphere. The heat loss cannot be greatly different from that in a well-mixed sphere, so that

$$q = \frac{12\sigma\bar{T}^4\gamma}{a\rho}. \tag{3.1}$$

4. According to Siedentopf's theory, as each convection unit rises it dissipates momentum by pushing matter aside and so experiences a resistance. Following Unsöld's account * a bubble of cross-section F moving upwards with a velocity ξ experiences a resistance of order $F\rho\xi^2$. The upthrust is $Fpgld\rho/\rho$, where l is the depth of the bubble. Unsöld sets $d\rho/\rho = -dT/T$ and equates upthrust to reaction, arriving at the approximate equation

$$\xi \approx \sqrt{gl\,dT/T}. \tag{4.1}$$

This gives a relation between two observables, the mean life of the granulation t and the contrast of the granulation which is a measure of dT/T. Unsöld advances reasons for supposing that l is the thickness of the convection zone, which he estimates at 500 km. Then with $dT/T = 2\cdot10^{-2}$ he gives $\xi = 1\cdot6$ km./sec. and $t = l/\xi = 314$ seconds. This agrees with the observed value 192 seconds obtained by Grotrian and ten Bruggencate.

We may here remark that if y is the ionization (of hydrogen),

$$\frac{d\rho}{\rho} = -\frac{dT}{T}\left(1 + \frac{T}{1+y}\left(\frac{\partial y}{\partial T}\right)_p\right) = -\gamma Q,$$

and that using Unsöld's basic data the value of Q is 2·3 at $\tau = 30$. However, the equation (4.1) is only approximate.

If we assume the velocity ξ known from equation (4.1) or its equivalent, then equations (3.1) (or (2.3)) and (1.1) give the radius of the granulation a and the temperature gradient. Strictly speaking a differential equation is involved and ξ is not necessarily constant with τ; but in the result the temperature gradients do not differ greatly from the radiative gradients, and reasonably consistent values of a are obtained by solving the ordinary equations at different depths. Further, a from (3.1) gives values of the right order of magnitude compared with observation. We conclude that ξ constant and the radiative (Milne) temperature gradient is a fair approximation to the actual phenomena.

We make numerical calculations from Unsöld's basic data given in *Physik d. Sternatmosphären*, p. 144, and choose the levels $\Theta = 0\cdot5$ (or $\tau = 11\cdot9$) and $\Theta = 0\cdot4$ (or $\tau = 30\cdot1$) as representing the convection zone. In place of (4.1) we use

$$\xi^2 = gl\gamma Q. \tag{4.2}$$

With an assumed value of ξ we can calculate γ from (4.2) and $dT/d\tau$ from (4.1) and then calculate a from (1.2) using either (2.4) or (3.1).

* *Physik d. Sternatmosphären*, p. 384, 1938.

Calculated Diameters of Convection Granules

$\Theta = 5040/T$	0·4			0·5		
ξ_1 km. sec.	4	3	2	4	3	2
γ from (4.2)	0·045	0·025	0·011	0·049	0·028	0·012
$2a$ from (3.1)	3″·81	2″·30	1″·41	3″·39	2″·05	1″·20
$2a$ from (2.4)	0″·12	0″·10	0″·08	0″·16	0″·12	0″·10

Although Plaskett gives 5″ as the mean size of the granula, ten Bruggencate gives 1″ to 2″. These values are supported by excellent photographs.* Accordingly a velocity between 2 and 3 km./sec. gives a good fit to the observed values judged by the calculations at both depths, and using the value of $2a$ found from (3.1). The temperature gradient is disturbed from the radiative value by 1 per cent. at both depths with $\xi = 2$ km./sec., and by 10 per cent. at $\Theta = 0{\cdot}4$, and 7 per cent. at $\Theta = 0{\cdot}5$ with $\xi = 3$ km./sec. Hence Unsöld's estimate of the lower limit of the convection zone will not be greatly in error and his value of 500 km. for the thickness of the convection zone may be accepted.

The mean life of the granulation is 167 sec. for $\xi = 3$ km./sec. and 250 sec. for $\xi = 2$ km./sec. (*cf.* Grotrian and ten Bruggencate's observed value of 190 sec.). Finally Unsöld gives 0·02 as the observed value of γ.

Bearing in mind the approximate nature of (4.2) and also the general uncertainty attached to our knowledge of basic solar data, particularly the absorption coefficient, the fit in $2a$ from (3.1) is extremely satisfactory and no further refinement of the theory is justifiable.

5. The theory gives no reason for the value of ξ. Eddington pointed out that the velocity of a particle falling freely under solar gravity through a distance equal to the depth of the convection zone was an extreme upper limit to ξ, and he suggested that 5 km./sec. was accordingly a "reasonable speed." It may be remarked that the velocity of sound in the convection zone is about 8 km./sec. and that presumably the resistance increases sharply as this velocity is approached, so that the velocity of sound is a limiting velocity. But these considerations only modify equation (4.1) and at present one condition is missing from the theory.

These limiting velocities, however, together with the observed value of γ, rule out the possibility of the temperature gradient approaching the adiabatic gradient. Inserting the adiabatic gradient in (1.1) we get $\xi\gamma = 5{\cdot}9 \times 10^4$ at $\Theta = 0{\cdot}4$ and $9{\cdot}4 \times 10^4$ at $\Theta = 0{\cdot}5$. Since γ depends on the fourth root of the observed contrast it is most unlikely that the observations are so much in error as to allow a value of γ twice that adopted by Unsöld, or $\gamma = 0{\cdot}04$. Taking the lower value of the product $\xi\gamma$ required by the adiabatic gradient we find $\xi = 15$ km. /sec. with the high value of γ. Much higher values of ξ are required at $\Theta = 0{\cdot}5$. Such high values of ξ are ruled out by the limiting conditions set out above, and this argument alone shows that the temperature gradients must be much closer to the Milne values than to the adiabatic values.

Commonwealth Solar Observatory,
Canberra:
1943 *February* 9.

* *Zs. f. Ap.*, 19, 59, 1939.

THE SHORT-PERIOD ERRATICS OF FREE PENDULUM AND QUARTZ CLOCKS

W. M. H. Greaves, F.R.S., and L. S. T. Symms

(Communicated by the Astronomer Royal)

(Received 1943 June 5)

Summary

The erratics of short period (derived from measures taken at intervals of one day) of clocks are discussed and three types of erratic are recognised. The first of these (type A) represents erratics of phase only, consisting of accidental fluctuations of phase, and also includes errors of chronographic recording and measurement. The third type (type C) represents erratics of rate only, consisting of accidental changes of rate.

The second or intermediate type of erratic (type B) may arise either from accidental fluctuations of rate about a mean value or from accidental changes of phase, the effects of these two kinds of erratic being indistinguishable. A method of analysis is given whereby a number is derived (the r-ratio) which indicates the degree of admixture of the three types of erratic.

It is found that for clocks of the standard free pendulum type all three types of erratic are present in appreciable amounts, but that for quartz clocks the erratics of types B and C are too small to be detected by the analysis and the erratics actually present are predominantly of type A. It is pointed out that type A erratics do not affect the long-period performance of a clock, but that the erratics of the other two types, especially those of type C, produce "wandering" of the clock by accumulation. It is accordingly concluded that in so far as the long-period performance of a clock arises from the integrated effects of the short-period erratics, good quartz clocks are very superior in long-period performance to the best clocks of the standard free pendulum type.

---

1. The investigation set forth in the present paper was carried out early in 1942. As far as the portion dealing with Shortt clocks is concerned, the material was the daily intercomparisons of three such clocks carried out at one of the stations responsible for the maintenance of the Greenwich time-service. A discussion of the relative performance of two quartz-controlled clocks at the National Physical Laboratory was included in the original discussion, which has now been supplemented by data relating to other quartz-controlled clocks.

The investigation deals with short-period erratics only, but it should be mentioned that recent developments tend to show that the superior performance of the best quartz-controlled clocks extends to long-term performance.

2. The short-period erratics of clocks can be conveniently studied by tabulating the measured daily changes of rate—that is, the second differences of the relative clock errors given by a series of chronographic comparisons taken regularly at 24-hour intervals. For a perfect clock running at a uniform rate these second differences would be all zero, and it would thus be expected that information as regards clock erratics would be obtained by forming the mean absolute second differences, that is, the mean measured daily changes of rate irrespective of sign, over any prescribed period, provided of course that this period is long enough to ensure that the results are statistically significant. This

procedure assumes that the second differences are of an accidental character, and this appears to be so apart from any tendency of the clocks concerned to exhibit a "curvature term" involving a continuous systematically positive or negative change of rate. Such a tendency is an undoubted feature of present-day precision clocks, whether they be pendulum clocks or whether they incorporate quartz vibrators, but in practice the systematic change of rate is less than one millisecond per day per day, and its effect upon the mean absolute second differences is negligible.

But a little consideration will show that a knowledge of the mean absolute second differences does not by itself give a true picture of the performance of clocks from the point of view of short-period erratics. It will be shown below, for example, that the mean absolute second differences of relative clock error for two particular quartz clocks is of the same order of magnitude as for two good Shortt clocks, but that the real nature of the erratics is essentially different in the two cases. It is necessary to discuss the various contributory causes which produce the variations in the second differences, and three such contributions have to be distinguished, viz.:

(*a*) Accidental erratics in the clock errors themselves arising from random fluctuations, about a mean value, of the phase at which the seconds impulses are taken, or from errors of chronographic recording and measurement.

(*b*) Accidental errors affecting the first differences. These may arise from accidental fluctuations of rate about a mean value or from accidental changes of phase.

(*c*) Accidental errors affecting the second differences arising from accidental changes of rate.

We shall refer to these three types of erratic as types A, B and C respectively.

It is important to realise the difference between erratics of type B arising from random fluctuations of rate, and erratics of type C arising from random changes of rate. In the first case the daily rates will be distributed in a random fashion about a mean value, but in the case of type C erratics there is no tendency for the rate to recover following a change. There is a similar distinction between erratics of types A and B arising from fluctuations of phase and changes of phase.

The distinction between the three types can be visualised by considering the effect of abnormally large isolated cases on a plot of clock error against time. The diagram shows the effect upon such a plot of isolated instances of the three types.

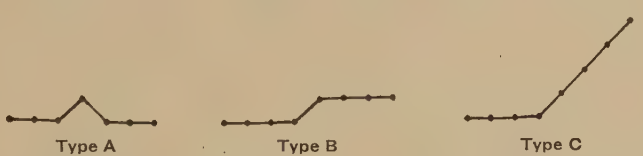

On studying actual examples of intercomparisons of clocks in which the daily differences of clock error are plotted against the calendar date, occasional extreme cases of all three types can be recognised. It should be noted that type B can arise from random changes of phase or random fluctuations of rate. Known causes of type A erratics in free pendulum clocks are the hit-and-miss action of slave synchronisers, erratic variations in the actions of the seconds switches whereby the time is taken off the slaves, and erratic variations in the actions of the free pendulum remontoire switches which control the slave synchronisers. Errors of chronographic recording and measurement are also included in type A.

Type B erratics can arise from fluctuations in the arcs of swing of a free pendulum arising possibly from variations in the intensity of impulsing. The origin of erratics of type C is obscure, but they undoubtedly exist in pendulum clocks and, from the point of view of long-period performance, are the most serious defects in modern precision clocks, as their effect on clock error is cumulative. Type B erratics also tend to produce

a cumulative effect on clock error, but they are less serious than type C as far as long-period performance is concerned.

From the foregoing it is clear that the tabulation of mean absolute second differences by themselves do not give a complete picture of performance, as they do not distinguish between the three types of erratic. It is possible, however, to get further information by tabulating an additional quantity as will now be shown.

3. Consider a series of chronographic comparisons between two clocks made at regular intervals (in the present investigation the intervals are 24 hours). Denote the differences of clock error thereby obtained by v_n.

Using a slightly modified form of the ordinary central difference notation, denote the first differences (daily rates) of the v_ns by $\delta_1 v_{n+\frac{1}{2}}$ and the second differences (daily changes of rate) by $\delta_1^2 v_n$.

Then

$$\delta_1 v_{n+\frac{1}{2}} = v_{n+1} - v_n \tag{1}$$

and

$$\delta_1^2 v_n = \delta_1 v_{n+\frac{1}{2}} - \delta_1 v_{n-\frac{1}{2}}, \tag{2}$$

so that

$$\delta_1^2 v_n = v_{n+1} - 2v_n + v_{n-1}. \tag{3}$$

Following up a suggestion which was originally due to Professor E. T. Whittaker, we write

$$\delta_2^2 v_n = v_{n+2} - 2v_n + v_{n-2}. \tag{4}$$

The quantities $\delta_1^2 v_n$ and $\delta_2^2 v_n$ are particular cases of more general expressions $\delta_m^2 v_n$, to which reference will be made below. All these quantities are of the same dimensions as the second differences $\delta_1^2 v_n$, which in the present investigation are given in milliseconds per day per day.

From (1), (2) and (4) the expressions for $\delta_2^2 v_n$ in terms of the first and second differences are

$$\delta_2^2 v_n = \delta_1 v_{n+\frac{3}{2}} + \delta_1 v_{n+\frac{1}{2}} - \delta_1 v_{n-\frac{1}{2}} - \delta_1 v_{n-\frac{3}{2}} \tag{5}$$

and

$$\delta_2^2 v_n = \delta_1^2 v_{n+1} + 2\delta_1^2 v_n + \delta_1^2 v_{n-1}. \tag{6}$$

Apart from systematic effects produced by acceleration, which in practice amount to less than one millisecond per day per day, and which are ignored in the present analysis, the quantities $\delta_1^2 v_n$ and $\delta_2^2 v_n$ possess the property that their algebraic averages over a sufficiently long period of time are zero. They are, however, not necessarily purely accidental series of quantities, since each $\delta_1^2 v_n$ is in general correlated with some of the preceding and following values, and similarly for the $\delta_2^2 v_n$s. We proceed to examine the way in which the $\delta_1^2 v_n$s and the $\delta_2^2 v_n$s are built up from the erratics of the three types.

We first consider erratics of type A which arise from purely accidental variations in the clock errors v_n, such as would be produced by accidental variations in the phase at which the time is taken from a pendulum, or by accidental errors of chronographic recording and measurement. The variations being purely accidental they are thus independent, there being no correlation between the erratic on a particular day and the erratics on the preceding and following days. The erratics contribute to the quantities $\delta_1^2 v_n$ and $\delta_2^2 v_n$, but these contributions do not form purely accidental series since the values are now correlated with some of the preceding and following values. From (3) it follows that $\delta_1^2 v_n$ involves v_n negatively and v_{n-1} positively, whereas $\delta_1^2 v_{n-1}$ involves v_n positively and v_{n-1} negatively, and this implies that there is a negative correlation between $\delta_1^2 v_n$ and $\delta_1^2 v_{n-1}$. Thus, for example, the effect of a positive type A erratic in v_n is to produce a negative contribution to the corresponding $\delta_1^2 v_n$ and a positive contribution to the immediately preceding second difference $\delta_1^2 v_{n-1}$. A negative erratic in v_{n-1} has the same effect. The statistical result is that if we select all the large negative values of $\delta_1^2 v_n$ it will be found that the mean of the immediately preceding

second differences $\delta_1^2 v_{n-1}$ is positive. Again, $\delta_1^2 v_n$ and $\delta_1^2 v_{n-2}$ both involve v_{n-1} positively so that there is a positive correlation between $\delta_1^2 v_n$ and $\delta_1^2 v_{n-2}$. Similarly there is a negative correlation between $\delta_1^2 v_n$ and $\delta_1^2 v_{n+1}$ and a positive correlation between $\delta_1^2 v_n$ and $\delta_1^2 v_{n+2}$. In the same way it follows from (4) that $\delta_2^2 v_n$ is correlated negatively with $\delta_2^2 v_{n-2}$ and $\delta_2^2 v_{n+2}$ and positively with $\delta_2^2 v_{n-4}$ and $\delta_2^2 v_{n+4}$.

We denote by $\pm\epsilon_a$ the mean absolute value (*i.e.* the mean value irrespective of sign) of the purely accidental variations of v_n which constitute the type A erratics. Then from (3) and (4) it follows that the resulting mean absolute values of $\delta_1^2 v_n$ and $\delta_2^2 v_n$ in a case in which type A erratics alone are operative are both $\pm\epsilon_a\sqrt{1^2+2^2+1^2} = \pm\sqrt{6}\epsilon_a$.

This application of the square rule of combining errors requires some justification since, as has been pointed out, the $\delta_1^2 v_n$ and $\delta_2^2 v_n$ are not series of independent accidental quantities. But if we divide the second differences into three sub-sequences, the first being $\delta_1^2 v_1$, $\delta_1^2 v_4$, $\delta_1^2 v_7$, etc., the second $\delta_1^2 v_2$, $\delta_1^2 v_5$, $\delta_1^2 v_8$, etc., and the third $\delta_1^2 v_3$, $\delta_1^2 v_6$, $\delta_1^2 v_9$, etc., then for each sub-sequence the values are independent accidental quantities and the mean absolute value for the sub-sequence will be $\pm\sqrt{6}\epsilon_a$. Accordingly the final mean absolute value for the whole sequence will also be $\pm\sqrt{6}\epsilon_a$. A similar argument applies to the $\delta_2^2 v_n$s.

It should also be noticed that we are tacitly assuming that the law of distribution of errors is such that mean absolute values can be combined by the square rule, as is the case for the Normal Error Law. From a strict theoretical point of view it would be more correct to use mean square values instead of mean absolute values. This would increase the labour of computation and it is exceedingly unlikely that any real advantage would be gained in the present application.

Next consider erratics of type B such as may arise from accidental fluctuations of clock rates about mean values or from accidental changes of phase. In this case the first differences are subject to purely accidental and independent variations. We denote the mean absolute value of these variations by $\pm\epsilon_b$. It then follows from (2) and (5) that in a case in which type B erratics are solely operative the mean absolute value of $\delta_1^2 v_n$ is $\pm\epsilon_b\sqrt{1^2+1^2} = \pm\sqrt{2}\epsilon_b$, and the mean absolute value of $\delta_2^2 v_n$ is $\pm\epsilon_b\sqrt{1^2+1^2+1^2+1^2} = \pm 2\epsilon_b$, the argument being justified by a division of the $\delta_1^2 v_n$ and $\delta_2^2 v_n$ into sub-sequences as before. There is again correlation between the neighbouring values of both $\delta_1^2 v_n$ and $\delta_2^2 v_n$.

Thirdly we consider type C erratics which arise from accidental changes of rate. When these are solely operative the second differences $\delta_1^2 v_n$ are purely accidental and independent quantities and we denote their mean absolute value by $\pm\epsilon_c$. From (6) it follows that the resulting mean absolute value of $\delta_2^2 v_n$ is $\pm\epsilon_c\sqrt{1^2+2^2+1^2} = \pm\sqrt{6}\epsilon_c$, the application of the square rule being again justified by the division of the $\delta_2^2 v_n$s into sub-sequences. The neighbouring values of $\delta_2^2 v_n$ are correlated.

In general all three types of erratic will operate simultaneously, and the individual $\delta_1^2 v_n$s and $\delta_2^2 v_n$s will be the sum of the resulting three components. Accordingly if we denote the mean absolute values of $\delta_1^2 v_n$ and $\delta_2^2 v_n$ by ϵ_1 and ϵ_2, we shall have in the general case

$$\epsilon_1^2 = 6\epsilon_a^2 + 2\epsilon_b^2 + \epsilon_c^2 \qquad (7)$$

and

$$\epsilon_2^2 = 6\epsilon_a^2 + 4\epsilon_b^2 + 6\epsilon_c^2, \qquad (8)$$

where ϵ_a, ϵ_b and ϵ_c are as have been defined, that is, they are respectively the mean absolute values of those components of v_n, $\delta_1 v_{n+\frac{1}{2}}$ and $\delta_1^2 v_n$ which are purely accidental and independent.*

* We have assumed that the erratics of the same type are mutually uncorrelated. It will be noticed that this implies no correlation between $\delta_1^2 v_n$ and $\delta_1^2 v_{n\pm p}$ for values of p greater than 2. This point has been tested for intercomparisons between three Shortt clocks using the same data as is analysed in section 4. For values of p from $p=3$ to $p=10$ the mean correlation coefficients obtained from the three sets of comparisons are all numerically less than $\pm 0{\cdot}10$ and appear to be accidental.

We now write

$$\epsilon_2/\epsilon_1 = r. \tag{9}$$

The quantity r is a measure of the degree of admixture of the three types of erratic. If erratics of type A are solely operative $r = 1$, if erratics of type B are solely operative $r = \sqrt{2} = 1{\cdot}41$, and if erratics of type C are solely operative $r = \sqrt{6} = 2{\cdot}45$. Accordingly a value of r near to unity will indicate that erratics of type A are predominant, and a value near to 2·45 will indicate that we are mainly concerned with erratics of type C. A value of r greater than 1·41 indicates that erratics of type C are certainly present.

It is necessary to notice the effect of erratics of types B and C on the relative clock errors v_n. If the only erratics present were of type A, a plot of relative clock error against calendar date would consist of a number of points scattered in a random manner about a straight line. Thus for comparisons at 24-hour intervals we should have $v_n = \alpha + n\beta + \epsilon_{a,\,n}$, where α is the initial value of the relative clock error apart from the erratic for day 0, β is the daily rate, and $\epsilon_{a,\,n}$ is the type A erratic for day n. But if type B erratics are also present, the erratic of this type in $\delta_1 v_{n+\frac{1}{2}}$ being denoted by $\epsilon_{b,\,n+\frac{1}{2}}$, then

$$v_n = \alpha + n\beta + \sum_{p=0}^{p=n-1} \epsilon_{b,\,p+\frac{1}{2}} + \epsilon_{a,\,n},$$

β being now the average value about which the daily rate fluctuates in an accidental fashion. The summation of the type B erratics in the expression for v_n produces a "wandering" in relative clock error, the smoothed plot of this against date being no longer a straight line.

If now type C erratics are superposed, the erratic of this type in $\delta_1{}^2 v_n$ being denoted by $\epsilon_{c,\,n}$, we have

$$v_n = \alpha + \sum_{p=0}^{p=n-1} \left[\left\{ \beta + \sum_{q=0}^{q=p} \epsilon_{c,\,q} \right\} + \epsilon_{b,\,p+\frac{1}{2}} \right] + \epsilon_{a,\,n}. \tag{10}$$

An equivalent form of (10) is

$$v_n = \alpha + n\beta + \sum_{p=0}^{p=n-1} [(n-p)\epsilon_{c,\,p} + \epsilon_{b,\,p+\frac{1}{2}}] + \epsilon_{a,\,n}. \tag{10'}$$

The expression (10) represents mathematically the physical conception of the three types of erratic*, namely that the actual rate on any day consists of accidental fluctuations (represented by the terms $\epsilon_{b,\,p+\frac{1}{2}}$) about a mean value $\beta + \sum_{q=0}^{q=p} \epsilon_{c,\,q}$ which itself is subject to the accidental changes which constitute the type C erratics.† In addition the phase at which the time is taken from the clock is subject to accidental fluctuations $\epsilon_{a,\,n}$ about a mean value. Just as we must distinguish between accidental fluctuations of rate about a mean value (type B erratics) and accidental changes of rate (type C erratics), so we must similarly distinguish between accidental fluctuations of phase about a mean value (type A erratics) and accidental changes of phase, the distinguishing feature of the latter (and of the accidental changes of rate) being that the several daily changes are independent, there being no correlation between the change on a given day and those

* But (10) is not a complete representation of clock performance, although it is a good approximation over a limited period of time. The curvature terms have been ignored, and in a long term discussion of performance they would have to be taken into account.

† The initial mean daily rate on day 0 is $\beta + \epsilon_{c,\,0}$. We may put $\epsilon_{c,\,0} = 0$, thereby defining β as the initial mean daily rate.

on the preceding and following days. But accidental changes of phase are indistinguishable in their effect from accidental fluctuations of rate, both of these erratics being represented by the accidental errors $\epsilon_{b,\,n+\frac{1}{2}}$ in the first differences. Accordingly they are both grouped together as erratics of type B. Erratics of type A also include the effect of accidental errors of chronographic recording and measurement.

We have so far been considering relative clock errors, obtained by chronographic comparisons of two clocks, but the same conceptions apply to the absolute errors of a single clock. These absolute errors can only be determined by transit observations, and if erratics of type A alone were present, a linear expression $\alpha+n\beta$ could be fitted to the transit observations over a considerable period of time, this expression being then capable of use for the extrapolation of the clock error over a correspondingly considerable period. In practice the type A erratics are of an order of magnitude smaller than the accidental errors of transit observations and so to a large extent they become immaterial. Under these circumstances the possibility of an extended linear extrapolation would provide a useful means of maintaining an accurate time-service over a prolonged period of cloudy weather when few transits are available.

But if erratics of types B and C are present in any appreciable degree, then, as a result of "wandering," the error accumulated by using a linear extrapolation of transit observations can rapidly exceed the limits of tolerance demanded from a first-class service, and this is especially true when appreciable erratics of type C are involved, there being a double summation of these erratics in the expression (10) for the clock error. It is thus a matter of importance to base the maintenance of a time-service on clocks for which the erratics of types B and C are as small as possible. Type C erratics represent the most objectionable defect in a precision clock.

The main object of any analysis of the kind indicated in this section is accordingly to compare the incidence of erratics of types B and C, and especially of type C, for different types of clock, the aim being to base the maintenance of a time-service on clocks for which the "wandering" produced by these types of erratic is least. In the succeeding sections the method of analysis will be applied to free pendulum and quartz clocks, and it will be seen that the latter are definitely much superior to free pendulum clocks, since for the quartz clocks the r-ratios are indistinguishable from unity whereas they are certainly greater than unity for clocks of the free pendulum type.

A practical point to which attention should be directed is that it will be found convenient to compute the quantities $\delta_2{}^2v_n$ from formula (6) and not from the equivalent form (4). This arises from the circumstance that the second differences $\delta_1{}^2v_n$ (which have to be formed in any case so as to obtain the mean absolute value ϵ_1) are comparatively small numbers in an actual case, and consequently the calculation of the $\delta_2{}^2v_n$s from formula (6) is convenient and comparatively rapid.

[Added 1943 June.] It has been remarked to us by Dr. H. R. Hulme that a more sensitive discrimination between the three types of erratic would be achieved by using, instead of $\delta_2{}^2v_n$, one of the higher members of the expressions

$$\delta_m{}^2v_n=v_{n+m}-2v_n+v_{n-m}. \qquad (11)$$

If we denote the mean absolute value of $\delta_m{}^2v_n$ by ϵ_m, then it can be verified that the general formula of which (8) is a particular case is

$$\epsilon_m{}^2=6\epsilon_a{}^2+2m\epsilon_b{}^2+\tfrac{1}{3}m(2m^2+1)\epsilon_c{}^2. \qquad (12)$$

If we now write

$$\epsilon_m/\epsilon_1=r_m, \qquad (13)$$

then if erratics of type A are solely operative $r_m=1$, if erratics of type B are solely operative $r_m=\sqrt{m}$, and if erratics of type C are solely operative $r_m=\sqrt{\tfrac{1}{3}m(2m^2+1)}$.

Clearly by taking higher values of m the values of r_m corresponding to the three types of erratic become more widely separated. Also the calculation of three of the quantities ϵ_m would permit of the complete derivation of the separate mean absolute erratics ϵ_a, ϵ_b and ϵ_c*, although this step would possibly only be justified for more extensive and more homogeneous sets of data than those subsequently analysed in this paper.

The tabulation of any series of the general expressions $\delta_m{}^2 v_n$ for $m > 2$ would increase the labour of computation which, as has been said, is comparatively rapid and convenient for $m = 2$. It has not been felt to be worth while to undertake the additional computations in the present instance. The investigation was primarily undertaken with the object of comparing the performances, from the point of view of short-period erratics, of free pendulum and quartz clocks, and, as will be seen, the simple analysis based on the use of the $\delta_2{}^2 v_n$s leads at once to the conclusion that quartz clocks are affected by erratics of types B and C to a very much smaller extent than is the case for pendulum clocks. This means that quartz clocks are much less affected by "wandering" than are pendulum clocks, and it seems likely that horology has now reached a stage at which for precision purposes existing types of pendulum clock will be replaced by clocks involving the use of vibrating quartz crystals. It is very improbable whether, at the present stage, justification could be found for the spending of undue time on a more elaborate investigation of the erratics of existing pendulum clocks.

But as soon as more extensive series of intercomparisons of quartz clocks become available, it would certainly be very worth while to embark on a more elaborate investigation of their erratics, and it is possible that improvements may be introduced into free pendulum clocks which would justify a careful discussion of the results obtained with the improved type. For the present, therefore, we have not attempted to extend the original discussion, and we confine ourselves to drawing attention to Dr. Hulme's remark which indicates how future analysis can be elaborated when the data justifies elaboration. In such an elaborated analysis it would probably be necessary to take into account the so-called curvature or acceleration terms which produce small systematically positive or negative values of the second differences. It may even be desirable to consider the possibility of erratic changes in the curvature terms, thereby bringing into consideration a fourth type of erratic which would produce purely accidental variations in the third differences.

4. *Discussion of Intercomparisons of Shortt Clocks.*—We proceed to apply this method of analysis to the intercomparisons between three Shortt clocks over the period 1941 August to December. The clocks are denoted by the letters X, Y and Z. Throughout this period these clocks have been intercompared twice a day within the hours before 10^h and 18^h U.T. The comparisons are reduced to 10^h and 18^h by application of the approximate daily rates. In the case of clock Z two slaves are controlled by the same free pendulum, one being a special slave, used to transmit the rhythmic signals radiated from Rugby, and called the "transmitter." The procedure has been to compare X and Y with the transmitter, these being the clock comparisons which are used to determine the error of the transmitter prior to setting it for the transmission of the radio signals. The error of the transmitter on each occasion is rectified by accelerating or retarding the whole Z ensemble, consisting of free pendulum, standard slave and transmitter, by the required amount, using magnetic correctors for this purpose, the total alteration per minute, when a prescribed current is passed through the correctors, having been measured. The times of passage of current through the correctors are recorded, and

* A more complete analysis would consist of plotting the quantities ϵ_m as functions of m for a number of values of m. This would, in principle, be an extension of the method introduced by Eddington and Plakidis (*M.N.*, 90, 65) and applied by them to a discussion of the irregularities of long-period variables.

in tabulating the data these records have been used to reduce comparisons involving Z to what they would have been if the correctors had never been used and the error of this clock never adjusted. In addition, regular comparisons have been made between the standard slave and transmitter of Z. As these are comparisons between two slaves controlled by the same free pendulum, they would be expected to show only erratics arising from phase variations, and this provides a check on the method of analysis.

The 10^h and 18^h series of clock comparisons have been analysed separately, and the results, meaned over the five months considered, are given in Table I, which gives the

TABLE I

Unit one millisecond/day²

	10^h Series			18^h Series		
	$\delta_1^2 v_n$	$\delta_2^2 v_n$	r	$\delta_1^2 v_n$	$\delta_2^2 v_n$	r
X/Z*t*	± 7·8	±12·0	1·54	± 8·8	±11·8	1·34
Y/X	9·3	16·9	1·82	10·6	15·1	1·42
Y/Z*t*	10·0	16·9	1·69	9·5	15·7	1·65
Z*s*/Z*t*	4·3	4·9	1·14	4·9	5·6	1·14

mean absolute values of $\delta_1^2 v_n$ and $\delta_2^2 v_n$ (these mean absolute values are the ϵ_1 and ϵ_2 of section 3) taken over the whole five months for the various intercomparisons. The values of r are also given.

The letters *t* and *s* attached to Z indicate whether the time is taken from the transmitter or from the ordinary slave.

It will be observed that for the comparisons involving Shortt clocks as a whole (free pendulums and slaves) the values of r range from 1·3 to 1·8, whereas for the comparisons Z*s*/Z*t*, in which two slaves under control of the same free pendulum are concerned, the value of r is much smaller. In this last case only phase variations enter, and there is no question of type C erratics being involved. The value of r found (1·14) is near to unity, indicating that the type A erratics (involving fluctuations of phase) are predominant. If the excess (0·14) over unity is real, it would imply that type B erratics (involving accidental changes of phase) are also present. The presence of erratics of type B would be expected to affect the difference between the two slaves by accumulation, thereby leading to a wandering of the difference apart from the day-to-day fluctuation due to erratics of type A. That this wandering actually does take place is shown by Table II, which gives for the 10^h and 18^h series separately the values of v_n for the comparisons between the two slaves (*i.e.* the phase difference between them) meaned over 10-day intervals. The data for the first week in 1942 January are included so as to complete the last 10-day group. An examination of the figures in this table shows that the wandering of phase between the two slaves is exhibited by each series independently. It will be noted that both series show a minimum at the interval September 30–October 9, a maximum towards the end of October, and a rise for the last 10-day interval.

The large difference in phase between the standard slave of clock Z and the transmitter was due to the circumstance that an attempt had been made to phase forward the transmitter by an amount approximately equal to the transmission time of the signals by land line to the radio station. This meant that the operation of the synchronising spring commenced when the pendulum of the transmitter was not in its central position,

TABLE II

Slave slow on Transmitter

10-day means

Unit one millisecond

	10^h	18^h		10^h	18^h
1941 Aug. 1–Aug. 10	102	101	1941 Oct. 20–Oct. 29	102	100
„ 11– „ 20	100	99	„ 30–Nov. 8	98	97
„ 21– „ 30	98	100	Nov. 9– „ 18	95	95
„ 31–Sept. 9	96	96	„ 19– „ 28	91	94
Sept. 10– „ 19	96	95	„ 29–Dec. 8	88	90
„ 20– „ 29	96	97	Dec. 9– „ 18	85	87
„ 30–Oct. 9	93	94	„ 19– „ 28	85	87
Oct. 10– „ 19	99	100	„ 29–Jan. 7	90	91

and it was subsequently felt that this was undesirable. The phasing was accordingly adjusted in 1942 April so that the synchronising arm engaged the spring when the pendulum was central. Although this adjustment has seemed to decrease the comparatively small number of occasions when difficulty was met in keeping the transmitter under its proper control by the master, analysis of the results obtained since the readjustment does not show any significant improvement. Over the four months 1942 September to December inclusive the average $\delta_1{}^2v_n$ for Zs/Zt was $\pm 4{\cdot}4$ and the average $\delta_2{}^2v_n$ $\pm 5{\cdot}5$, giving $r = 1{\cdot}25$. The phase differences obtained by 10-day means ranged from 68 to 49 milliseconds,* this range of 19 milliseconds being comparable with, and actually slightly greater than, the range of the values in Table II.

The results for the clock intercomparisons, which have been summarised in Table I, are given in a different form in Table III. In this table the mean absolute values of

TABLE III

Unit one millisecond/day²

	X/Zt			Y/X			Y/Zt			Zs/Zt		
	$\delta_1{}^2v_n$	$\delta_2{}^2v_n$	r	$\delta_1{}^2v_n$	$\delta_2{}^2v_n$	r	$\delta_1{}^2v_n$	$\delta_2{}^2v_n$	r	$\delta_1{}^2v_n$	$\delta_2{}^2v_n$	r
1941 Aug.	±11·9	±16·0	1·34	±10·4	±15·8	1·52	±12·4	±20·6	1·66	±5·8	±6·4	1·10
Sept.	6·2	9·8	1·58	8·4	15·8	1·88	8·4	15·4	1·83	3·8	4·9	1·29
Oct.	6·6	9·0	1·36	11·9	20·1	1·69	13·0	22·1	1·70	4·5	5·0	1·11
Nov.	10·1	13·5	1·34	11·4	17·4	1·53	8·2	12·0	1·46	4·1	5·1	1·24
Dec.	6·7	11·2	1·67	7·5	10·8	1·44	6·6	11·6	1·76	4·8	4·8	1·00
Means	± 8·3	±11·9	1·43	± 9·9	±16·0	1·62	± 9·7	±16·3	1·68	±4·6	±5·2	1·13

$\delta_1{}^2v_n$ and $\delta_2{}^2v_n$ for the 10^h and 18^h series have been meaned and the results are grouped according to calendar months. It will be seen that for the comparisons involving free pendulums as well as slaves there is a distinct variation from month to month in the mean absolute values of $\delta_1{}^2v_n$ and $\delta_2{}^2v_n$ and in the ratios r. It seems that the erratics of the three types are variable in amount from time to time, and that consequently the

* It should be noticed that the centring of the synchronising units of two slaves under the control of the same free pendulum does not necessarily produce a recorded phase difference of zero, since the recorded phase difference includes the differences of adjustment and operation of the two seconds switch mechanisms.

mean values in the last row of the table must be taken as representing average performance over the five months considered. At the same time it appears from Table I, in which the average values for the 10^h and 18^h series are given separately, that the agreement between the two series is good and that consequently the final means have a statistical significance.

But for the comparisons between the two slaves Zs and Zt, which are both controlled by the same master, the accordance of the figures from month to month is good, indicating that we are here dealing with erratics which are more homogeneous with respect to time. In particular the monthly values of the r-ratios are more accordant for the comparisons between these two slaves. This is probably due to the circumstance that the effect of erratics of one type (type A) is here predominant.

The final mean absolute values of $\delta_1{}^2v_n$ and $\delta_2{}^2v_n$ for the comparisons between Y and X and between Y and Z (transmitter) are practically the same. This means that the performance of X and Z are the same, and accordingly we can get the mean absolute values of $\delta_1{}^2v_n$ and $\delta_2{}^2v_n$ for either by dividing the values for the comparisons between them by $\sqrt{2}$. We thus get for either of these clocks $\delta_1{}^2v_n = \pm 8{\cdot}3/\sqrt{2} = \pm 5{\cdot}9$ and $\delta_2{}^2v_n = \pm 11{\cdot}9/\sqrt{2} = \pm 8{\cdot}4$, giving $r = 1{\cdot}42$. And for the comparison of either with Y we have $\delta_1{}^2v_n = \pm 9{\cdot}8$ and $\delta_2{}^2v_n = \pm 16{\cdot}2$, so that for Y alone we have

$$\delta_1{}^2v_n = \pm\sqrt{(9{\cdot}8)^2 - (5{\cdot}9)^2} = \pm 7{\cdot}8 \quad \text{and} \quad \delta_2{}^2v_n = \sqrt{(16{\cdot}2)^2 - (8{\cdot}4)^2} = \pm 13{\cdot}9,$$

giving $r = 1{\cdot}78$.

We thus get the following values for the three clocks:—

TABLE IV

	$\delta_1{}^2v_n$	$\delta_2{}^2v_n$	r
X, Zt	±5·9	± 8·4	1·4
Y	±7·8	±13·9	1·8

The high value of the r-ratio for clock Y suggests that the inferior performance of this clock, as indicated by the value $\pm 7{\cdot}8$ for $\delta_1{}^2v_n$, is due, in part at least, to the increased incidence of erratics of type C. Now type C erratics must be purely properties of free pendulums, and it accordingly would be of interest if we could separate the effects of the slaves and obtain results appertaining to the free pendulums alone. We can do this by assuming that the performances of all slaves are the same, in which case the mean absolute values of $\delta_1{}^2v_n$ and $\delta_2{}^2v_n$ for any slave are obtained by dividing the results for the comparisons Zs/Zt by $\sqrt{2}$.

This gives for a slave:

$$\delta_1{}^2v_n = \pm 4{\cdot}6/\sqrt{2} = \pm 3{\cdot}3,$$
$$\delta_2{}^2v_n = \pm 5{\cdot}2/\sqrt{2} = \pm 3{\cdot}7.$$

We can now deduce results appertaining to the free pendulums alone. Thus for the free pendulums of X and Z we get $\delta_1{}^2v_n = \pm\sqrt{(5{\cdot}9)^2 - (3{\cdot}3)^2} = \pm 4{\cdot}9$. In this way we get the results given in Table V.

TABLE V

Results for Free Pendulums

	$\delta_1{}^2v_n$	$\delta_2{}^2v_n$	r
X, Z	±4·9	± 7·5	1·5
Y	±7·1	±13·4	1·9

Taking Table V as a correct representation of the free pendulum performances, the question arises whether any erratics of type A are still present. Such erratics could

only enter into the performance of a free pendulum as a result of a variable action of the switch which provides the synchronising currents controlling the slaves. If the time elapsing between the instant at which the gravity arm leaves the impulse wheel mounted on the free pendulum and the instant at which the switch arm makes contact (thereby sending out the synchronising signal and at the same time operating the free pendulum remontoire) be variable, type A erratics will be introduced.

We proceed to deduce values of ϵ_a, ϵ_b and ϵ_c for the free pendulums from the data in Table V on two hypotheses which probably represent extremes. In the first place let us assume that the free pendulum switch is perfect and introduces no erratics of type A. The mean absolute values of $\delta_1{}^2v_n$ and $\delta_2{}^2v_n$ given in Table V can then be used to deduce the separate values ϵ_b and ϵ_c for the erratics of types B and C by solving equations (7) and (8) of section 3 with ϵ_a put equal to zero. This gives the following results for the free pendulums:—

	Free Pendulums X and Z	Free Pendulum Y	
ϵ_a	0	0	
ϵ_b	$\pm 3{\cdot}3$	$\pm 3{\cdot}9$	msecs./day
ϵ_c	$\pm 1{\cdot}4$	$\pm 4{\cdot}4$	msecs./day^2

Secondly, let us assume that the free pendulum switch introduces the same type A erratics as are introduced by the slaves. We have found that for a single slave $\delta_1{}^2v_n = \pm 3{\cdot}3$ and $\delta_2{}^2v_n = \pm 3{\cdot}7$. Solving with $\epsilon_c = 0$, this gives $\epsilon_a = \pm 1{\cdot}2$ and $\epsilon_b = \pm 1{\cdot}2$. We thus assume $\epsilon_a = \pm 1{\cdot}2$ for free pendulums and again solve from the data in Table V. There results:

	Free Pendulums X and Z	Free Pendulum Y	
ϵ_a	$\pm 1{\cdot}2$	$\pm 1{\cdot}2$	msecs.
ϵ_b	$\pm 2{\cdot}4$	$\pm 3{\cdot}2$	msecs./day
ϵ_c	$\pm 2{\cdot}1$	$\pm 4{\cdot}7$	msecs./day^2

Since the slaves cannot introduce erratics of type C, it follows that a value of ϵ_c found for a free pendulum will apply to the clock as a whole. It will be noticed that in both solutions the type C erratics (as indicated by the value of ϵ_c) are enhanced for clock Y, as is indeed shown by the high values of r for this clock in Tables IV and V. These erratics would be expected to influence the long-period performance of the clock owing to the cumulative nature of their effect, and it is in fact true that the long-term performance of Y, as shown by plots of its error derived from transit observations, is inferior to that of either of the other two clocks.

It is well known that when the errors of free pendulum clocks, as determined by transit observations, are plotted over an interval of several months, the fact emerges that these clocks are liable to occasional large changes of rate which may exceed 10 milliseconds per day. The question arises as to whether these occasional large changes of rate can be regarded as extreme cases of the normal type C erratic or whether they are to be classed separately as occasional catastrophic changes in the clock. There seems to be no reason for regarding the occasional large changes of rate as anything more than extreme cases of erratics of type C. If we assume in the first place that for a good clock erratics of this type contribute a mean absolute daily change of rate amounting to $\pm 1{\cdot}4$ msecs./day^2 (this being the value of ϵ_c found above for clocks X and Z on the first limiting assumption that the free pendulum itself does not contribute to type A erratics), then the probable error of the daily change of rate is $\pm 1{\cdot}4 \times {\cdot}8453 = \pm 1{\cdot}2$. The probable error of the accumulated change of rate in say five days is $\sqrt{5}$ times this or $\pm 2{\cdot}7$, and assuming a normal frequency distribution, this means that the probability that a change of rate amounting to more than 10 milliseconds per day will develop in any given five-day interval is 1/80, leading to an expectation of about one such change in a

year. The accidental errors of transit determinations of clock error being what they are, a change of rate of this kind, developing in five days, would, if transit observations were taken as the sole criterion of performance, be interpreted as an instantaneous change of rate.

If, however, we take $\epsilon_c = \pm 2{\cdot}1$ msecs./day^2, this being the value found for clocks X and Z on the second limiting assumption that the free pendulums contribute equally with the slaves to the total type A erratics, a similar calculation gives an expectation of about six or seven changes of rate per year exceeding 10 msecs./day over a five-day interval.

As regards the actual performances of clocks X and Z over the period 1941 August to December, an examination of transit plots and plots of clock comparisons showed that the change of rate accumulated in five days by these two clocks exceeded 10 msecs./day on one and four occasions respectively in the five-month period. This, for what it is worth, seems to favour the second hypothesis, namely that the free pendulums contribute equally with the slaves to type A erratics. But evidence of this kind should not be stressed, as the excess of the number of actual changes of rate over the expectation calculated on the basis of $\epsilon_c = \pm 1{\cdot}4$ may be a result of sampling error and of the well-known tendency in experimental data for extreme errors to be more frequent than is predicted by the normal Law of Errors. It should be noticed that when the erratics of type C are small the calculated expectation is very sensitive to the exact value of ϵ_c used.

For clock Y the values of ϵ_c of $\pm 4{\cdot}4$ and $\pm 4{\cdot}7$ found above lead respectively to expectations over five months of thirteen and fourteen changes of rate exceeding 10 msecs./day and developing in five days. The actual number of such changes for 1941 August to December found by the examination of transit plots and clock comparisons was ten.

Owing to the various processes to which the mean values of $\delta_1^2 v_n$ and $\delta_2^2 v_n$ given in Table III have been subjected, stress must not be laid on the exact numerical values obtained above, and the results must be regarded as indicative of order of magnitude only. The conclusion seems to emerge that for good Shortt clocks, of which X and Z may be regarded as examples, the average daily changes of rate represented by type C erratics are of the order of magnitude of one or two milliseconds per day per day. For a clock such as Y the type C erratics are more pronounced. It has, unfortunately, not so far proved possible to associate the occurrence of enhanced erratics of this type with any particular kind of mechanical defect.

It is perhaps necessary to point out that the method of analysis used above, although possessing the advantage of discriminating between the three types of erratics discussed, cannot be expected to lead in itself to a complete picture of the performance of the clocks. One well-known feature of Shortts which is ignored by the analysis is the systematic acceleration often found—that is, a systematic tendency to a change of rate of the same sign persisting for periods of months at a time. Such "curvature terms" seem to be always less than one millisecond per day per day, and it has accordingly been possible to ignore them in the present investigation. Their origin is unknown, and one of the puzzling features about them is their comparatively sudden appearance, their persistence over a period of months, and then their disappearance or comparatively sudden change of value. Like the erratics of type C, curvature terms are probably associated with some particular mechanical features in the clocks, but in neither case has the origin of the disturbance been traced.

5. *Results for Quartz Clocks.*—It is of interest to compare the results obtained for Shortt clocks with corresponding results using the same method of analysis for quartz clocks, these consisting of phonic motors controlled *via* frequency dividers by vibrating quartz crystals. There are two such clocks (Q2 and Q6) at the National Physical Laboratory, and the time of reception of the Rugby 10^h signal is recorded daily on each of them. These measures, which are forwarded to Greenwich among other recipients,

have been used for the derivation of intercomparisons between the two clocks. But this set of data is not as satisfactory for statistical purposes as the Shortt clock intercomparisons discussed in the preceding section. In the first case only one series (at 10^h U.T.) is available, whereas for the Shortt clocks there was the 18^h series as well. There have been occasions when the 10^h signal from Rugby was not radiated, leading to gaps in the data. Further, Q6 stopped on 1941 Septenber 17 and Q2 on October 28.

The unsatisfactory nature of the data makes it all the more remarkable that the intercomparisons between the two quartz clocks give very consistent results, as is shown by Table VI.

TABLE VI

Intercomparisons of Quartz Clocks

Unit one millisecond/day²

Q2/Q6

	$\delta_1{}^2v_n$	$\delta_2{}^2v_n$	r
1941 Aug. 14–Sept. 17	±10·4	± 9·6	0·92
Sept. 19–Oct. 27	8·1	8·3	1·02
Oct. 29–Nov. 30	8·2	9·1	1·11
Dec. 1–Dec. 31	10·0	10·3	1·03
Means	± 9·2	± 9·3	1·01

The outstanding feature of the results is that the value of r is very close to unity. This means that the erratics must be predominantly of type A, and on comparison with Table III it appears that this predominance is actually more pronounced for the intercomparison of the two quartz clocks than for the case of two Shortt slaves (*Zs* and *Zt*) under the control of the same free pendulum.

The mean absolute value of $\delta_1{}^2v_n$ is $\pm 9{\cdot}2$ for the quartz clock intercomparisons. Assuming that this is equally distributed between the two clocks, we get for each $\delta_1{}^2v_n = \pm 9{\cdot}2/\sqrt{2} = \pm 6{\cdot}5$. Assuming that the whole of this is due to erratics of type A, we get for the mean absolute variation in phase combined with the mean absolute error of chronographic recording and measurement the value $\epsilon_a = \pm 6{\cdot}5/\sqrt{6} = \pm 2{\cdot}7$ milliseconds. Genuine phase variations could conceivably arise from erratic action of the commutator switches by which the seconds signals are taken from the phonic motors, and it is possible that errors of chronographic recording and measurement contribute to the total type A erratics.

In so far as long-term performance is the result of the accumulation of short-period erratics of type C and, to a lesser extent, of type B, it would appear that for quartz clocks it should be very good. From the data given in Table VI it does not seem likely that the value of r for the intercomparison between the two quartz clocks exceeds 1·05. A value of r less than 1·05 combined with a mean absolute $\delta_1{}^2v_n$ equal to $\pm 9{\cdot}2$ means that $\epsilon_c < 1{\cdot}4$ msecs./day², and so for a single quartz clock the mean absolute value of the type C erratics would be less than $\pm 1{\cdot}4/\sqrt{2} = \pm 1{\cdot}0$ milliseconds per day per day. This represents a performance comparable to, and probably better than, the very best pendulum clocks.

When the long-term performance of quartz clocks is assessed by comparison with transit observations it transpires that, like clocks of the free pendulum type, they possess curvature terms indicating a progressive continuous change of rate. This feature is especially prominent for Q6. It also appears that sudden large changes of rate can take place. In the cases of the two quartz clocks here considered there were no large sudden changes of rate during the five months covered by the investigation, but Q6 changed rate on 1942 January 20–21 and Q2 on 1942 February 23–24. In the case of Q6 the clock suddenly commenced to run faster by about 30 msecs./day, and the change

in Q2 was about 20 msecs./day in the opposite sense. These changes of rate are far too large to be regarded as extreme cases of normal type C erratics (which, as we have seen, must be very small for quartz clocks) and must be regarded as comparatively rare catastrophic changes in the periods of vibration of the crystals.

[Added 1943 April]

Some further information as to the performance of quartz clocks is given by three clocks at the Post Office Radio Branch Laboratories. These clocks are designated IV A, IV B and IV C, and the times of reception of the Rugby 10^h signals on them have been forwarded to Greenwich. Analysis of recent data gives the figures in Table VII.

TABLE VII

Intercomparison of P.O. Quartz Clocks 1942 *December* 11–1943 *March* 30

Unit one millisecond/day²

	$\delta_1^2 v_n$	$\delta_2^2 v_n$	r
IV A/IV B	±7·1	±7·1	1·00
IV B/IV C	5·7	5·6	0·98
IV C/IV A	5·2	5·3	1·02

Again the values of r are close to unity, indicating that the erratics are predominantly of type A. It will be noticed that the mean absolute values of $\delta_1^2 v_n$ and $\delta_2^2 v_n$ are smaller than was the case in Table VI, indicating that for the P.O. clocks the erratics are smaller. It will also be noticed that the values for IV A/IV B are larger than for the comparison of either of these clocks with IV C, indicating that the erratics of IV C are smaller. As far as the erratics of type A are concerned, it appears that IV C is at least comparable to the best pendulum clocks and probably better than any of them. These erratics of type A do not of course affect the long-period performance of the clocks concerned by accumulation. But when we come to erratics of types B and C the great superiority of these quartz clocks over clocks of the pendulum type is very clear.

We are indebted to the Director of the National Physical Laboratory and to the Head of the Post Office Radio Department for their kind permission to utilise the results of quartz clock intercomparisons in the above discussion.

ON SOME OPTICAL SYSTEMS EMPLOYING ASPHERICAL SURFACES

E. H. Linfoot

(Received 1943 May 17)

Summary

General formulæ for the Seidel errors, excluding distortion, of optical systems consisting of two figured mirrors and one figured plate are obtained by the "See-saw diagram" method of Dr. C. R. Burch. These are applied to discuss the possibility of dispensing with the figuring on the mirrors, and it is shown that the only flat-fielded anastigmat with both mirrors spherical is equivalent to the field-flattened Schmidt. Finally, the equations are used to design a flat-fielded aplanat consisting of two spherical mirrors and one aspheric plate, and its performance is estimated.

---

1. An elegant and attractive method of discussing the Seidel errors of a centred optical system has recently been described by Dr. C. R. Burch.* Briefly stated, its principle is as follows: Any spherical (reflecting or refracting) surface can be anastigmatised by an aspherical plate located at its centre of curvature. The Schmidt camera, which consists of a single spherical mirror together with an anastigmatising plate, is the simplest example. In an optical system S involving several spherical surfaces, we should annul the first four Seidel errors (*i.e.* all except distortion) if we could provide each surface with its anastigmatising plate of the correct strength and in the correct position. For then the successive imagings by the different surfaces would be free from the first four Seidel errors and so therefore would their resultant. To carry this out in practice it would be necessary that the light, in its transit between each surface of the system S and the corresponding anastigmatising plate, should not encounter any further surface of the system. Most systems fail to satisfy this condition. However, it is easily verified that if an aspherical plate is replaced by its image † in that part of the system which precedes it (in the sense of light travel), its effect on the Seidel errors is unchanged. We may therefore image all the plates associated with S through on to the object side, and obtain a set of plates, of known strengths and positions, which together would annul the first four Seidel errors of the system S. Reversing the strengths of each of these plates, we obtain a set of plates which, taken together with the entry-pupil of S, form an optical system whose first four Seidel errors agree with those of S. The fifth Seidel error (distortion) can also be treated by this method, but it is no longer true that the set of plates (with signs reversed) reproduces the distortion of the original system, and supplementary considerations relating to the projection of spherical image surfaces on to each other have to be introduced.

It is not necessary that the object should be at infinity, but when it is the analysis of the plate-system takes an especially simple form, and by means of a simple graphical representation (called the "see-saw" diagram by Dr. Burch in his account of the method) it is possible to get a clear mental picture of the effect on off-axis image quality of changes in the constants of the system S. Since it covers the first four Seidel errors, the method,

* *M.N.*, **102**, 159, 1942.

† The image of a plate is here defined as follows: its position and lateral size are found by Gaussian optics, while the angular deviation which it imparts to the rays passing through it at each point is to be the same after transformation as before.

used together with Petzval's theorem and Conrady's 3 : 1 rule, suffices to determine the field curvature of the system S.

2. We shall apply the method to give a general discussion of the properties of systems consisting of two mirrors and a nearly plane parallel plate. Flat-fielded anastigmats of this pattern have been proposed by Dr. James G. Baker (*J. Amer. Phil. Soc.*, **82**, 339, 1940) and by Dr. Burch (*loc. cit.*). To obtain flat-fielded anastigmatism it is in general necessary that at least two of the optical surfaces shall be aspherical (see section 5 below for the only exception to this statement). Special practical interest, however, attaches to the case where both mirrors are spherical and only the correcting plate is figured. For such a design would be no more difficult to construct than an ordinary Schmidt camera and could have the advantage of an accessible image surface. We show that such a design cannot be strictly anastigmatic, so that a price must be paid for the accessible field. Secondly, we show that its field curvature can be satisfactorily controlled, and pick out a flat-fielded system suitable for use as an astrographic camera. Lastly, we set out some computational results which give an estimate of the performance of the system as compared with that of Schwarzschild's two-mirror aplanats.*

3. Consider two spherical mirrors of radii $\rho_1 = 2f_1$ (concave), $\rho_2 = 2f_2$ (convex), with

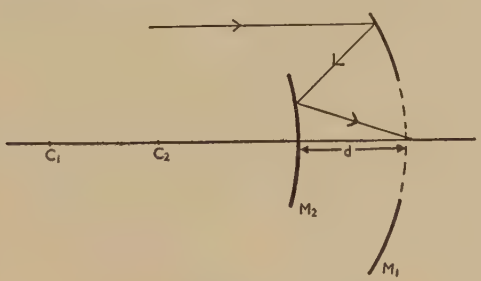

FIG. 1.

the axial points of their surfaces spaced d apart. Let C_1, C_2 be their centres. Rays parallel to the axis entering from the left (Fig. 1) will be focussed on the axis at a distance $\frac{f_2(f_1-d)}{d+f_2-f_1}$ in front of the convex (*i.e.* to its right). Thus $f_1 - f_2 \leqq d \leqq f_1$ is the condition for a real image. This image will lie behind the concave mirror (*i.e.* to its right) if $d^2 + d(2f_2 - f_1) - f_1 f_2 < 0$, *i.e.* if

$$0 \leqq d \leqq \sqrt{\tfrac{1}{4}f_1^2 + f_2^2} + \tfrac{1}{2}f_1 - f_2.$$

This is the condition for an "accessible" image.

The convex mirror is working with paraxial distances

$$u = -(f_1 - d), \qquad v = f_2(f_1 - d)/(d + f_2 - f_1),$$

where we agree to measure distances from a mirror positively in front of it, negatively behind it. Thus the magnification $\lambda = \frac{v}{u} = -\frac{f_2}{d+f_2-f_1}$. The surface deformation needed to remove its spherical aberration would be $(\lambda-1)^2/(\lambda+1)^2$ times parabolic correction. If this were done on a plate at the centre of curvature (ignoring for the moment the physical impossibility of this) the diameter of the plate would have to be $(\rho_2 - u)/u = \frac{\lambda-1}{\lambda+1}$ times

* Attention should here be drawn to an important paper of H. Slevogt (*Z. für Instrumentenkunde*, 1942 October). Slevogt gives a very complete survey of the Schmidt and its variants, of the two-mirror aplanats, and of the Baker anastigmats. He draws attention to a flat-fielded aplanat closely similar to that investigated in sections 9, 10 below, and points out that its astigmatism is so small that it may for practical purposes be regarded as anastigmatic. His paper includes a very full bibliography.

that of the mirror. So the plate would need strength $(\lambda+1)^4/(\lambda-1)^4$ times what it would have needed if it had been the same diameter as the mirror, *i.e.* $+\left(\frac{\lambda+1}{\lambda-1}\right)^4\left(\frac{\lambda-1}{\lambda+1}\right)^2$ times parabolic correction, *i.e.* $-\left(\frac{\lambda+1}{\lambda-1}\right)^2 = -\left(\frac{f_1-d}{d+2f_2-f_1}\right)^2$ times Schmidt plate strength S_2 for a (concave) sphere of radius ρ_2. The light could not actually reach such a plate; therefore we replace it by its image in the part of the system which precedes it, namely, the concave mirror. It is imaged at a distance $f_1(2f_2+d)/(d+2f_2-f_1)$ in front of the concave and with magnification $f_1/(d+2f_2-f_1)$. Thus the image-plate has its strength increased in the ratio $\left(\frac{d+2f_2-f_1}{f_1}\right)^4$, to the value

$$-\frac{(f_1-d)^2(d+2f_2-f_1)^2}{f_1^4}S_2.$$

Since this plate is in fact not present, we conclude that the contributions of the convex mirror to the first four Seidel errors of the system (for an object at infinity) agree with those arising from a plate of strength $\{-(f_1-d)^2(d+2f_2-f_1)^2/f_1^4\}S_2$ situated at a distance $f_1(2f_2+d)/(d+2f_2-f_1)$ in front of the concave.

In the same way, the contributions of the concave mirror to the first four Seidel errors would be annulled by a Schmidt plate placed at its centre of curvature and of strength S_1 corresponding to its radius of curvature. Hence the contributions from the mirror alone agree with those from a plate of strength $-S_1$ situated $2f_1$ in front of it.

Now the strength of a Schmidt plate for a sphere of radius ρ is proportional to $1/\rho^3$. Thus if we take as deformation-unit the strength of a Schmidt plate for a sphere of radius $2(f=1)$ we have

$$S_1 = 1/f_1^3, \qquad S_2 = 1/f_2^3.$$

We have thus determined the plate system corresponding to our system of two spherical mirrors. Now suppose that the mirrors are not spherical, but figured. In the domain of third-order optics such figurings can be represented as constant multiples of parabolic correction and imaged through the system to the object side, where they contribute additional members to the plate system. The figuring (of strength α say) on the concave mirror images into itself. That on the convex mirror contributes a plate (of strength β say) located $df_1/(f_1-d)$ behind the concave mirror. The strength of the actual figuring on the concave mirror is then $\left(\frac{f_1}{f_1-d}\right)^4\beta$.

Lastly, suppose that the system includes a glass aspherical plate, of strength γ, located at a distance x in front of the concave mirror. We can abolish this plate at will by setting $\gamma=0$. Then the plate system consists of five components:

(1) Located $df_1/(f_1-d)$ behind the concave mirror, a plate of strength β (image of the figuring on the convex).

(2) Located *on* the concave, its own figuring, of strength α.

(3) Located $\frac{f_1(2f_2+d)}{d+2f_2-f_1}$ in front of the concave, a plate of strength

$$+\frac{(f_1-d)^2(d+2f_2-f_1)^2}{f^4f_2^3}$$

(image of the anastigmatising plate which the convex lacks, with sign reversed).

(4) Located $2f_1$ in front of the concave, a plate of strength $-1/f_1^3$ (Schmidt plate which the concave lacks, with sign reversed).

(5) Located x in front of the concave, a glass aspherical plate of strength γ.

Conditions for Anastigmatism.—These are invariant under stop-shifting, so we may take the stop on the surface of the concave. Then the system has the "plate diagram" shown in Fig. 2, distances being measured from the stop position as origin and taken as positive against the light.

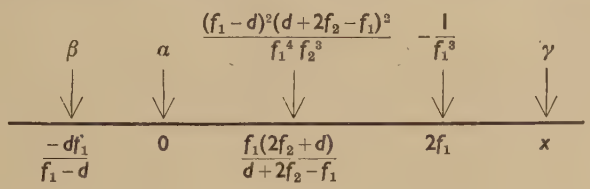

FIG. 2.

The conditions for anastigmatism are accordingly:

(spherical aberration) $$\alpha+\beta+\gamma+\frac{(f_1-d)^2(d+2f_2-f_1)^2}{f_1^4f_2^3}-\frac{1}{f_1^3}=0, \tag{1}$$

(coma) $$+\frac{df_1}{d-f_1}\beta+x\gamma+\frac{f_1(2f_2+d)}{d+2f_2-f_1}\frac{(f_1-d)^2(d+2f_2-f_1)^2}{f_1^4f_2^3}-\frac{2}{f_1^2}=0, \tag{2}$$

(astigmatism) $$\left(\frac{df_1}{f_1-d}\right)^2\beta+x^2\gamma+\frac{f_1^2(2f_2+d)^2}{(d+2f_2-f_1)^2}\frac{(f_1-d)^2(d+2f_2-f_1)^2}{f_1^4f_2^3}-\frac{4}{f_1}=0. \tag{3}$$

When these are satisfied, the field curvature is equal to the Petzval curvature, viz. $1/f_1-1/f_2$.

4. *Anastigmat from Two Spheres and One Plate* (concave primary mirror).—This is the case $\alpha=\beta=0$.

The anastigmatism conditions (1), (2), (3) become

$$\gamma=\frac{1}{f_1^3}-\frac{(f_1-d)^2(d+2f_2-f_1)^2}{f_1^4f_2^3}, \tag{4}$$

$$x\gamma=\frac{2}{f_1^2}-\frac{(2f_2+d)(f_1-d)^2(d+2f_2-f_1)}{f_1^3f_2^3}, \tag{5}$$

$$x^2\gamma=\frac{4}{f_1}-\frac{(2f_2+d)^2(f_1-d)^2}{f_1^2f_2^3}. \tag{6}$$

These give, eliminating x and γ,

$$\left(\frac{4}{f_1}-\frac{(2f_2+d)^2(f_1-d)^2}{f_1^2f_2^3}\right)\left(\frac{1}{f_1^3}-\frac{(f_1-d)^2(d+2f_2-f_1)^2}{f_1^4f_2^3}\right)=\left(\frac{2}{f_1^2}-\frac{(2f_2+d)(f_1-d)^2(d+2f_2-f_1)}{f_1^3f_2^3}\right)^2,$$

i.e.

$$\frac{[(2f_2+d)-2(d+2f_2-f_1)]^2(f_1-d)^2}{f_1^5f_2^3}=0,$$

giving $d=2f_1-2f_2$ or $d=f_1$, as necessary conditions. Thus *a system consisting of two spherical mirrors and one aspherical plate can only be anastigmatic in two cases:*

(1) *When the spheres are concentric.*

(2) *When the second sphere is at the paraxial focus of the first.*

Case (2): $d=f_1$.—Then the only effect of the second sphere is to change the field curvature. Equations (4), (5), (6) become

$$\gamma=1/f_1^3, \qquad x\gamma=2/f_1^2, \qquad x^2\gamma=4/f_1;$$

thus

$$x=2f_1, \qquad \gamma=S_1,$$

and the system is simply a Schmidt with changed field curvature. Its field curvature, being equal to its Petzval curvature, is $1/f_1 - 1/f_2$. Thus flat-fieldedness is achieved when $f_2 = f_1$. In practice we should replace the convex ("field-flattening") mirror by a field-flattening *lens*, in contact with the photographic plate, of focal length *

$$\{(2n+1)/n\}f \simeq \tfrac{8}{3}f.$$

Case (1): $d = 2f_1 - 2f_2$ (concentric spheres).—Equations (4) and (5) become

$$\gamma = \frac{1}{f_1^3} - \frac{(2f_2 - f_1)^2 f_1^2}{f_1^4 f_2^3}, \qquad x\gamma = \frac{2}{f_1^2} - \frac{2f_1(2f_2 - f_1)^2}{f_1^2 f_2^3},$$

giving $x = 2f_1$. Thus the glass aspherical plate goes at the centre of curvature of the concave, but its strength γ is not $S_1 = 1/f_1^3$ but

$$S_1\left(1 - \frac{(2f_2 - f_1)^2 f_1}{f_2^3}\right).$$

To get this strength down to zero, and so dispense with the aspherical plate, we should need

$$i.e. \qquad f_2^3 = (2f_2 - f_1)^2 f_1, \qquad f_2/f_1 = 1, \qquad \frac{3 \pm \sqrt{5}}{2}. \tag{7}$$

$f_2/f_1 = 1$ gives spheres in contact; $f_2/f_1 = (3+\sqrt{5})/2$ gives $f_2 > f_1$, which is physically impossible. Thus the only two-sphere anastigmat with concave primary, convex

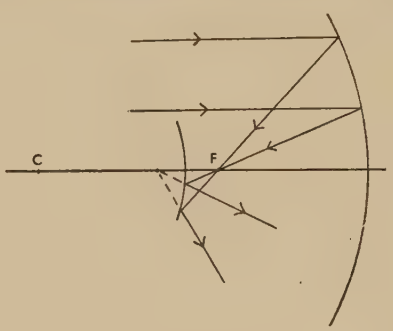

Fig. 3.

secondary, is that given by

$$f_2 = \frac{3-\sqrt{5}}{2} f_1 = 0{\cdot}3820 f_1, \qquad d = (\sqrt{5} - 1)f_1 = 1{\cdot}2361 f_1$$

and shown in Fig. 3. Since $d > f_1$ the image is virtual; it is formed at a distance $(5-\sqrt{5})f_1/2 = 1{\cdot}3819 f_1$ in front of the concave mirror. The focal length

$$f = f_1 f_2/(f_2 - f_1 + d) = \frac{\sqrt{5}-1}{2} f_1 = \tfrac{1}{2}d = 0{\cdot}6181 f_1.$$

The Petzval radius is f, since the system is monocentric.

5. *Systems with Convex Primary and Concave Secondary Mirror.*—The general plan of these systems is shown in Fig. 4. The only change needed in the analysis is the

* This is the "extended paraxial" value, *i.e.* the value when aperture and field are small. It decreases rather rapidly when the aperture and field-diameter are increased. At a focal ratio of $f/1$ and for a field of 20° diameter, where we are nearing the limits beyond which field-flattening by this method becomes impracticable, the focal length of the field flattener falls to about $\frac{5}{8}f$.

substitution of $-f_1$, $-f_2$ for f_1, f_2. Thus the new plate diagram (taking the stop on the primary, now the convex, mirror) is as shown in Fig. 5.

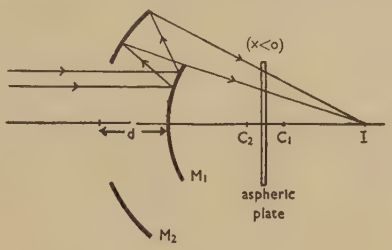

FIG. 4.

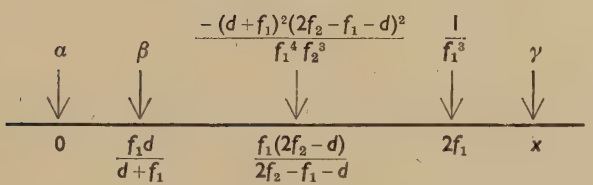

FIG. 5.

In the case of two spheres ($\alpha=\beta=0$) and one plate, anastigmatism is now only possible if $d=-2f_1+2f_2$, *i.e.* if the spheres are concentric. (The other solution of section 4 now becomes $d=-f_1$, which is physically impossible). In this case $x=-2f_1$ and the plate has to go in a physically impossible position *behind* M_1. If we try to get round this difficulty by imaging it in one or both mirrors, it always remains at their common centre C. Thus the plate must lie in a rather strongly converging beam, and its adjustment will be very troublesome. Only in the case $\gamma=0$ do we get a workable system, therefore. This case, by section 4 with $-f_1$, $-f_2$ for f_1, f_2, is when

$$-f_2^3=-(2f_2-f_1)^2 f_1, \qquad f_2/f_1=1, \qquad \frac{3\pm\sqrt{5}}{2}.$$

$f_2/f_1=1$ gives spheres in contact as before; $f_2/f_1=\dfrac{3-\sqrt{5}}{2}$ gives $f_2<f_1$, which is physically impossible. Thus the only two-sphere anastigmat with convex primary, concave secondary, is that given by

$$f_2=\frac{3+\sqrt{5}}{2}f_1=2{\cdot}6181f_1, \qquad d=(\sqrt{5}+1)f_1=3{\cdot}2361f_1.$$

The image is real and is formed at a distance $6{\cdot}1771f_1$ from the concave. The focal length

$$f=\frac{f_1 f_2}{f_2-f_1-d}=\frac{\sqrt{5}+1}{2}f_1=\tfrac{1}{2}d=1{\cdot}6181f_1.$$

The Petzval radius is f.

We conclude from sections 4, 5, that:

The only flat-fielded anastigmat obtainable with two spherical surfaces and one aspherical plate is the field-flattened Schmidt. (In practice, M_2 will here be replaced by a field-flattening *lens*, in order that a photographic plate placed in the image surface may receive the light).

The only anastigmats obtainable with two spherical surfaces alone are the monocentric systems described above, of which only the second produces a real image.

6. *Two-Sphere Aplanats.*—If in the conditions (4), (5), (6) of section 4 we retain only (4), (5) and in them put $\gamma = 0$, we obtain the conditions for a two-sphere aplanat, namely

$$\frac{1}{f_1^3} = \frac{(f_1 - d)^2(d + 2f_2 - f_1)^2}{f_1^4 f_2^3}, \qquad \frac{2}{f_1^2} = \frac{(2f_2 + d)^2(f_1 - d)^2(d + 2f_2 - f_1)}{f_1^3 f_2^3}.$$

By allowing f_1, f_2 to take both positive and negative values, we cover the cases both of convex and concave mirrors under one head; $f_1 > 0$, $f_2 > 0$ means a concave primary and a convex secondary mirror.

The equations give first $f_1 \neq d$ and then

$$2(d + 2f_2 - f_1) = 2f_2 + d,$$
$$d = 2f_1 - 2f_2.$$

Thus the spheres must be concentric, and (eliminating d)

$$f_2^3 = (2f_2 - f_1)^2 f_1,$$

which, as we have seen, is also the condition for anastigmatism. Thus: *the only 2-sphere aplanats are the two 2-sphere anastigmats.* It is easy to prove this directly from the plate diagram, by first proving the system monocentric.

7. *The Seidel Error-Coefficients (except Distortion) in Terms of the Plate Diagram.*—An aplanatising plate for a sphere of radius 2 ($f = 1$) has surface equation $\xi = \beta h^4$, $\beta = \frac{1}{3\frac{1}{2}}(n - 1)$, n being the refractive index. Its "optical equation" is $\eta = (n - 1)\beta h^4$, where η stands for optical path-length, normalised to zero on the axis. Thus $\eta = \frac{1}{3\frac{1}{2}} h^4$ is the "optical equation" of a plate of unit strength.

For a sphere of radius $2f_1$, the plate strength is $S_1 = 1/f_1^3$ units and the optical equation $\eta = \frac{1}{3\frac{1}{2}} S_1 h^4$. The lateral deviation imposed by such a plate on rays traversing it nearly normally at height h is thus $\frac{1}{8} S_1 h^3$ in circular measure. Now consider plates

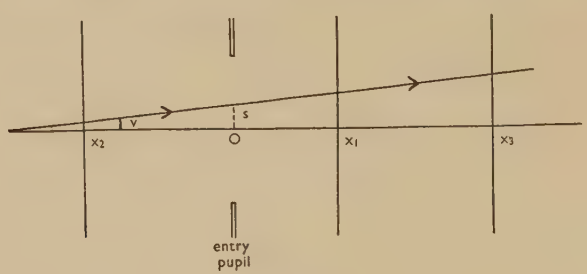

FIG. 6.

of strengths $a_1, a_2 \ldots \gtrless 0$ at distances $x_1, x_2 \ldots \gtrless 0$ from the entry pupil of our system, as shown in Fig. 6. (It is evidently possible for plates to occupy positions in front of the entry pupil; for such plates $x < 0$.)

The angular deviation of a meridional ray, passing the stop at a distance S from its centre and making an angle v with the axis, is (to the third order)

$$\tfrac{1}{8}\sum_i a_i(s + vx_i)^3 = \tfrac{1}{8}s^3\sum_i a_i + \tfrac{3}{8}s^2 v\sum_i a_i x_i + \tfrac{3}{8}sv^2\sum_i a_i x_i^2 + \tfrac{1}{8}v^3\sum_i a_i x_i^3. \qquad (8)$$

Therefore the Seidel coefficients B, F, C of the optical system which possesses the above as its plate system are given by the equations *:

---

* Contrast the well-known equation

$$\Delta = Bs^3 - 3Fs^2 v + (2C + D)sv^2 - Ev^3$$

for the "deviation" of the intersection *with the Gaussian image plane* of a meridional ray.

$$B = -\tfrac{1}{8}\sum_i \alpha_i \quad \text{(spherical aberration)}, \tag{9}$$

$$F = +\tfrac{1}{8}\sum_i \alpha_i x_i \quad \text{(coma)}, \tag{10}$$

$$C = -\tfrac{1}{8}\sum_i \alpha_i x_i^2 \quad \text{(astigmatism)}. \tag{11}$$

The fourth term $\frac{1}{8}v^3\Sigma\alpha_i x_i^3$ is connected with the distortion, but does not itself measure the distortion of the system, since additional distortions originate in the field curvatures of the anastigmatised surfaces. To obtain the Seidel coefficient D, we use the equation

$$2(D-C) = \text{Petzval curvature of the system} = \Sigma \pm 1/f_i$$

in the case of a system consisting of mirrors and aspherical plates, the summation being over the mirrors. The field curvature is then

$$C + D = 2C + (D-C) = -\tfrac{1}{4}\sum_i \alpha_i x_i^2 + \tfrac{1}{2}\sum \pm 1/f_i.$$

8. *Astigmatism of Two-Mirror-Plus-Plate Aplanats.*—The off-axis astigmatism of a thin lens centrally passed, or of a spherical mirror, is given by the equation

$$\text{Distance between centres of astigmatic focal lines} = \delta^2/f,$$

where f is the focal length and δ the displacement of the image off axis. It is sometimes convenient to express the astigmatism of a composite system as a fraction of that of a thin lens (or of a spherical mirror) of the same focal length. For a sphere of focal

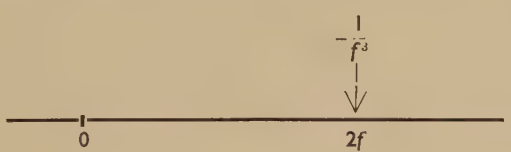

FIG. 7.

length f, imaging from infinity with entry-pupil at the mirror-surface, the plate diagram is given by Fig. 7.
Thus for such a sphere, by section 7,

$$B = \frac{1}{8f^3}, \qquad F = -\frac{1}{4f^2}, \qquad C = \frac{1}{2f},$$

and C has this same value for any centrally passed thin lens. Therefore the "thin lens value" of C is $1/2f$ and the astigmatism of a system of focal length f is

$$2fC = -\tfrac{1}{4}f\sum_i \alpha_i x_i^2$$

times the thin lens value. The distance between the centres * of the astigmatic focal lines (or "astigmatic focal distance") of the system at displacement δ off-axis is therefore

$$-\frac{\delta^2}{f} \cdot \tfrac{1}{4}f\sum_i \alpha_i x_i^2 = -\tfrac{1}{4}\delta^2\sum_i \alpha_i x_i^2,$$

where α_i, x_i refer to its plate diagram.

* In the domain of third-order optics, the lengths of the astigmatic focal lengths are third-order small quantities, while their distance apart is a second-order small quantity. Thus it is also legitimate to speak simply of the "distance between the astigmatic focal lines," with the same meaning as above.

We can apply this formula to express the off-axis astigmatism of the general two-mirror-plus-plate aplanat in terms of the thin lens value or of the astigmatic focal distance.

The focal length $f=f_1f_2/(f_2-f_1+d)$ in the first type (concave primary). The value of $\sum_i \alpha_i x_i^2 = -8C$ is, in an aplanatic system, independent of the stop-position. (A direct proof of this result, and so of the invariance of astigmatism in an aplanat under stop-shifting, follows at once from equations (8) to (11).) Taking the stop on the primary, we have by section 3

$$\sum_i \alpha_i x_i^2 = \left(\frac{df_1}{f_1-d}\right)^2\beta + x^2\gamma + \frac{(2f_2+d)^2(f_1-d)^2}{f_1^2f_2^3} - \frac{4}{f_1},$$

and this equation consequently holds for all positions of the stop.

The astigmatism coefficient C is $-\frac{1}{8}\times$ this quantity, or

$$\frac{-f_1f_2}{4(f_2-f_1+d)}\left\{\left(\frac{df_1}{f_1-d}\right)^2\beta + x^2\gamma + \frac{(2f_2+d)(f_1-d)^2}{f_1^2f_2^3} - \frac{4}{f_1}\right\}$$

times the thin lens value, and the astigmatic focal distance is

$$-\tfrac{1}{4}\delta^2\left\{\left(\frac{df_1}{f_1-d}\right)^2\beta + x^2\gamma + \frac{(2f_2+d)^2(f_1-d)^2}{f_1^2f_2^3} - \frac{4}{f_1}\right\} \qquad (12)$$

at distance δ off-axis. To obtain the corresponding formulæ for systems of the second type (convex primary) we have only to replace f_1, f_2 by $-f_1$, $-f_2$.

9. *Flat-Fielded Aplanats.*—We next ask whether it is possible to construct a high-definition flat-fielded aplanat from two spherical mirrors and one aspherical plate. We also demand that the image shall be "fully accessible," *i.e.* outside the optical system.

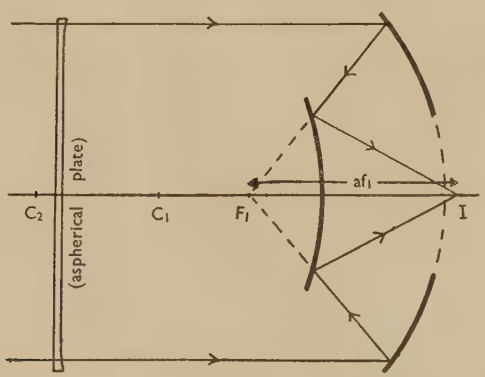

Fig. 8.

Fig. 9.

We specify that type of flat-fieldedness in which the tangential, sagittal and Petzval curvatures are in the ratios 2 : 4 : 5 and the plate meets the tangential focal surface at the edge of the field (see Fig. 9). This is the type appropriate to systems (such as those used in astronomical photography) where only very slight imperfections of the image can be tolerated. The specification

$$1/\rho_T : 1/\rho_S : 1/\rho_P = 2 : 4 : 5 \qquad (13)$$

is equivalent to

$$C : D : D-C = -1 : 4 : 5, \qquad (14)$$

where in the general case

$$C = -\tfrac{1}{8}\sum_i \alpha_i x_i^2 = -\tfrac{1}{8}\left\{\left(\frac{df_1}{f_1-d}\right)^2 + x^2\gamma + \frac{(2f_2+d)^2(f_1-d)^2}{f_1^2 f_2^3} - \frac{4}{f_1}\right\}$$

$$D - C = -\tfrac{1}{2}\left(\frac{1}{f_1} - \frac{1}{f_2}\right).$$

The condition for flat-fieldedness in the general case is thus

$$-\tfrac{1}{4}\left\{\left(\frac{df_1}{f_1-d}\right)^2\beta + x^2\gamma + \frac{(2f_2+d)^2(f_1-d)^2}{f_1^2 f_2^3} - \frac{4}{f_1}\right\} = \tfrac{1}{5}\left(\frac{1}{f_1} - \frac{1}{f_2}\right), \tag{15}$$

together with the aplanatism conditions (1), (2).

Case of Two Spheres and Plate ($\alpha = \beta = 0$).—Then (1), (2) reduce to (4), (5) and conditions become (4), (5) and

$$x^2\gamma = \frac{4}{f_1} - \frac{(2f_2+d)^2(f_1-d)^2}{f_1^2 f_2^3} + \tfrac{4}{5}\left(\frac{1}{f_1} - \frac{1}{f_2}\right). \tag{16}$$

Eliminating x, γ we obtain as a necessary condition

$$\left[\frac{4}{f_1} - \frac{(2f_2+d)^2(f_1-d)^2}{f_1^2 f_2^3} + \tfrac{4}{5}\left(\frac{1}{f_1} - \frac{1}{f_2}\right)\right]\left[\frac{1}{f_1^3} - \frac{(f_1-d)^2(d+2f_2-f_1)^2}{f_1^4 f_2^3}\right]$$

$$= \left[\frac{2}{f_1^2} - \frac{(2f_2+d)(f_1-d)^2(d+2f_2-f_1)}{f_1^3 f_2^3}\right]^2$$

which reduces to

$$-(d+f_2-f_1)^2 = \tfrac{1}{5}\frac{f_2-f_1}{f_1 f_2}\left\{\frac{f_1^2 f_2^3}{(f_1-d)^2} - f_1(d+2f_2-f_1)^2\right\}. \tag{17}$$

For any solution (f_1, f_2, d) of this, the values of x, γ are given by (4), (5) and the system is then completely determined. It still remains to discuss its physical properties, of course.

We here digress for a moment to remark that if the type of flat-fieldedness desired were that in which the sagittal and tangential focal surfaces have equal and opposite curvatures, the only change needed would be the replacement in (15) and (17) of the factor $\frac{1}{5}$ by $\frac{1}{2}$, and that any of the other standard types of field-flattening may be expressed by altering this factor to a new and easily calculated value.

Change of Notation.—Equation (17) is homogeneous in the variables f_1, f_2, d. We therefore introduce the new variables $\xi = f_2/f_1$, $q = 1 - d/f_1$ and obtain (17) in the form

$$\xi q^2(\xi - q)^2 = \tfrac{1}{5}(\xi - 1)(\xi^3 - q^2(2\xi - q)^2),$$

i.e.

$$f(q) \equiv (4\xi+1)q^4 - 2\xi(2+3\xi)q^3 + \xi^2(\xi+4)q^2 - \xi^3(1-\xi) = 0. \tag{18}$$

The left-hand side, considered as a function of q alone, has stationary values at

$$q = 0, \qquad q = \xi, \qquad q = \frac{\xi(\xi+4)}{2(4\xi+1)}.$$

In a type 1 system $0 < \xi < 1$, and it is easily shown that

$$f(0) = -\xi^3(1-\xi) \leqq 0, \qquad f(\xi) = -\xi^3(1-\xi)^2 \leqq 0,$$

while as $q \to \pm\infty$, $f(q) \to \infty$. It follows that $q = 0$, ξ are minima and $q = \xi(\xi+4)/2(4\xi+1)$ is a maximum. Whether equation (18) has two real roots in q or four therefore depends on whether $f(q) \lesseqgtr 0$, for $q = \xi(\xi+4)/2(4\xi+1)$. Its value there is

$$\frac{\xi^3}{16(4\xi+1)^3}\{5\xi^2(\xi+4)^3 - 16(1-\xi)(4\xi+1)^3\}.$$

Now in the range $0 \leqq \xi \leqq 1$ the equation

$$5\xi^2(\xi+4)^3 - 16(1-\xi)(4\xi+1)^3 = 0$$

has just one root, namely $\xi = 0{\cdot}710\ldots$ Thus for $0{\cdot}710\ldots < \xi \leqq 1$ the quartic $f(q) = 0$ has four real roots in q, for $0 \leqq \xi < 0{\cdot}710$ only two. The *first* root is always $\leqq 0$, the second and third (when real) lie between 0 and ξ, while the fourth is greater than ξ, since ξ is a minimum value of $f(q)$. See Fig. 10. All possible type I flat-fielded aplanats are derived from these roots, and each root leads to a type I flat-fielded aplanat, but some of these may be physically impracticable or valueless. To clear up this point we have to discuss the position of the image.

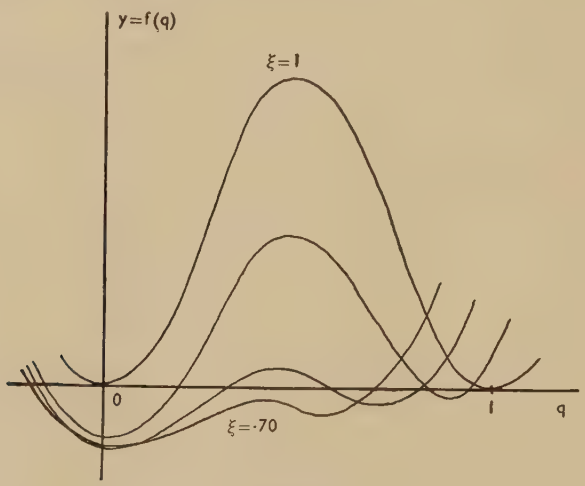

Fig. 10.

Image Accessibility.—Let

$$a = \frac{IF_1}{f_1} = \frac{\xi q}{\xi - q} + q.$$

Then the condition for a "fully accessible" image—that is, one formed behind the concave primary—is that a should be somewhat greater than 1, say $a \geqq 1{\cdot}1$. The condition for a *real* image is $a \geqq q$, *i.e.* $\xi q/(\xi - q) + q \geqq q$, which is equivalent to $0 \leqq q < \xi$. Thus only the second and third roots can yield a practicable system, and consequently only values of ξ in the range $0{\cdot}710\ldots \leqq \xi \leqq 1$ come into consideration.

Plotting values of a from the second and third roots of $f(q) = 0$ against values of the parameter ξ, we see from Fig. 11 that to obtain an astrographic camera we should always use the second root.

ξ	a (2nd root)	ξ	a (2nd root)
0·71	1·558	0·73	1·034
0·72	1·141	0·75	0·866

Since $a = 1{\cdot}034$ is a little on the small side (because of the thickness of the primary and its mounting), the best choice therefore lies between $\xi = 0{\cdot}72$ and 0·73, so far as image position alone is concerned. But off-axis astigmatism also must be considered. We obtain, using the formula of section 8, the table

ξ	a	Astig./Thin Lens Value
0·72	1·141	−·161
·73	1·034	−·143
·75	0·866	−·113

from which it is clear that the astigmatism does not change very rapidly with ξ. Hence we may take $\xi = 0{\cdot}72$ as the most suitable value. The constants of the flat-fielded aplanat which results are (normalising with $f_1 = 1$)

$$a = 1{\cdot}1411; \quad d = 0{\cdot}6281; \quad f_2 = 0{\cdot}7200;$$

$$\gamma = 1 - \frac{q^2(2\xi - q)^2}{\xi^2} = 0{\cdot}5773 \text{ (plate strength)};$$

$$x = 2{\cdot}047 \text{ (plate position)}; \quad f = \xi/(\xi - q) = 2{\cdot}068.$$

Its general appearance is shown in Fig. 8. For a system of nominal aperture-ratio $F/2$, the plate radius is 0·517. In the case of an $F/2$ Schmidt of the same focal length (say $f = 2$)

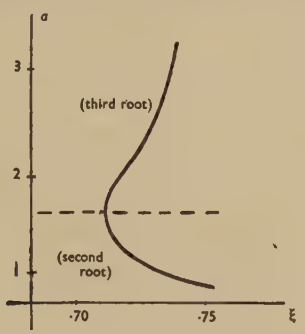

FIG. 11.

the plate strength would be 1/8. Thus our aplanat requires a plate 4·618 times as strong as does a field-flattened Schmidt of the same focal length and aperture.

10. *Practical Usefulness of the System.*—A straightforward calculation shows that the secondary mirror obscures the whole of the aspherical plate as seen from any point of a $\pm 7\frac{1}{2}^\circ$ field surface. Thus the photographic plate is shielded from direct illumination and the system can be used as a daylight camera.

To form an estimate of the off-axis image quality, meridional pencils were traced through the system and the radial spreads in the best field (taken as the plane through the tangential constrictions of the pencils at the edge of the field demanded) determined for the on-axis pencil. These spreads agree, on the Seidel theory, with the greatest diameters of the confusion-ellipses in the field, and Väisälä's ray-traces of modified Schmidt cameras indicate that in a system of this F-number and angular field the Seidel values will lie fairly close to the true values. The final result is that for a field of $\pm 2^\circ$ the error spreads amount to 1′ of arc in a system of nominal aperture $F/2$ (effective aperture $F/3$). In the Schwarzschild two-mirror aplanats, which employ two aspherical mirrors and have an "inaccessible" image position (*i.e.* one between the two mirrors), the radial spread of meridional edge rays at $F/3{\cdot}3$ and 1°·5 off-axis was 18″ (agreeing well with Seidel theory). To compare these results we must find what the corresponding spreads of a Schwarzschild aplanat of effective aperture $F/3$ (*i.e.* nominal aperture $F/2{\cdot}6$) would be at 2° off-axis. They would be

$$\left(\frac{2}{1{\cdot}5}\right)^2 \times \frac{3{\cdot}3}{2{\cdot}6} \times 18'' = 40'' \text{ nearly.}$$

Thus our system gives error-spreads 3/2 times larger than those of Schwarzschild's aplanat. It seems probable that applications exist in which its greater ease in construction and greater convenience in use will considerably outweigh this optical inferiority.

Bristol University:
1943 *May* 15.

GRADIENTS AND COLOUR TEMPERATURES OF γ CASSIOPEIÆ

D. L. Edwards

(Received 1943 June 7)

Summary

Colour-temperature observations of γ Cass have been made during the period 1938 June to 1941 October, using objective-prism spectra of γ and δ Cass.

The method is described and the results tabulated and discussed in relation to accompanying spectrum changes.

The possibility is also discussed of a relation between gradient and the number of Balmer emission lines in the spectrum; but any such relation, though pronounced during one stage of the stars' outburst, does not appear to be permanent.

A series of observations of γ Cass was started in 1938 with the object of determining its colour temperature at frequent intervals from objective-prism spectra, but the reduction of the plates was postponed pending the development of a suitable technique for such work. This use of objective-prism spectra was first suggested by Professor W. H. M. Greaves, and after careful consideration a tentative scheme, suited to the equipment available at Sidmouth, was formulated. This scheme has been thoroughly investigated by D. R. Barber *, who applied it to stars in the Greenwich † list of standards, and found it to give very satisfactory results after determining quantitatively the various errors inherent in such work or eliminating them by adjustments of the procedure. The details of this method, which are fully described by Barber, are summarised in the following paragraphs, with some modifications designed to meet the special case of γ Cass.

The instrument used was the 12-inch McClean prismatic camera, stopped down to 4 inches aperture to give convenient exposure times, and adjusted to give the spectrum in good focus at regions near $H\alpha$ and $H\gamma$. It has a dispersion of about 32 A./mm. at $H\gamma$. Fast panchromatic plates were used, specially made by Ilford and sensitive to approximately 7000 A. These were standardised with a tube sensitometer ‡, using Wratten blue and red filters 47*a* and 71*a*. These filters have fairly narrow ranges of transmission in wave-length, with maxima very close to the centres of the two spectral regions measured, and the method was found experimentally by Barber to give results equal to that from monochromatic standardisation (from a step-wedged spectrum) at the exact wave-lengths used.

The comparison star used was δ Cass, and although this was found to be a variable by Guthnick and Prager §, the range of magnitude is very small (0·07) and it is probably of Algol type, so that there appears to be no objection to using it for a gradient comparison. There is no reason to suspect a temperature variation, and the star was, in fact, chosen at Greenwich as one of their standards. It was also used later at that observatory as a comparison for γ Cass.

The spectra of γ and δ were taken close together on one plate, which was then

* Unpublished.

† *Obs. of Colour Temperatures of Stars, 1926–32*, 1932.

‡ *N.L.O. Bull.* No. 1, 14, 1938.

§ *V.J.S.*, 51, 79, 1916.

immediately standardised and developed. The exposure times required to give spectra of similar density for the two stars were almost the same, while the *effective* exposures in these trailed spectra (*i.e.* the total exposure divided by the number of strips contained in the whole spectrum of width equal to that of a stationary image) was identical with the exposure time given in the sensitometer. Thus no correction was needed for reciprocity failure of the emulsion. Photographs were, as far as possible, taken only on the best nights, when there was no moonlight or other source of general fog, and no mist or haze, so that the "fog effect" * was negligible and atmospheric extinction was made as small as possible. The actual values used for the extinction were those specially determined for Sidmouth by Barber in the work mentioned.

The plates were measured in the "Oxford" microphotometer †, using direct readings of the galvanometer deflections, and the method of reduction was based on that used at Greenwich. Intensities were measured at six different wave-lengths in the red region and at six in the blue, and the means of each group taken as the intensities at the two mean wave-lengths. The exact positions used at Greenwich were not suitable for this work as some of them fell on or very near bright lines in the γ Cass spectrum. In order to choose the best positions some large-scale microphotometer tracings were made of the two regions, and wave-lengths selected where the background appeared to be free from the influence of either absorption or emission lines in both stars. This procedure was repeated when any change in γ Cass suggested the possibility of new lines appearing, and any slight necessary adjustments were made, without affecting the mean wave-lengths appreciably. Such adjustments were rarely needed, and in the majority of cases the following positions were found to be satisfactory:—

Red: 6176, 6215, 6273, 6295, 6395, 6423 A.
Blue: 4155, 4194, 4211, 4239, 4266, 4279 A.

giving the mean wave-lengths of the two regions as ·6296 μ and ·4244 μ, with

$$\Delta(1/\lambda) = 0{\cdot}7791.$$

If I is the intensity in δ and I' in γ, with suffixes B and R indicating the blue and red regions, then the gradient difference is given by

$$\Delta\phi = \frac{\log_e (I_R/I_R') - \log_e (I_B/I_B')}{\Delta(1/\lambda)} = 2{\cdot}956 \log_{10} (I_R I_B'/I_B I_R').$$

This gradient difference needed correction by the addition of the differential atmospheric extinction for the two stars (which was always within the range −·029 to +·048), and the relative gradient, G, of γ Cass was then obtained by adding 0·25, the gradient of δ Cass relative to the Greenwich zero point. Finally the absolute gradient, ϕ, was obtained by assuming the value 1·00 for the Greenwich zero.

An estimation of the probable errors of observation was obtained by plotting the measured gradients against dates of observation and drawing a freehand curve, made to follow the large-scale variations of ϕ (the reality of which was confirmed by contemporary spectrum changes) but ignoring minor changes. The deviations of the plotted points from this mean curve gave a probable error of ±0·02. This should represent an upper limit to the value of the probable error, and the actual value is probably rather less than this as a fraction of the scatter round the mean curve may be due to real changes in the gradient of γ Cass. The probable error is thus about the same as that of Greenwich ‡, where the average probable error was found to be ±0·02 for catalogue stars and ±0·013 for standard stars.

The results are given in the table, where ΔG is the gradient difference between γ and δ (in the sense γ − δ) after correcting for atmospheric extinction, ϕ the absolute

* *M.N.*, 100, 529, 1940. † *N.L.O. Bull.* No. 2, 20, 1939. ‡ *M.N.*, 100, 189, 1940.

gradient of γ, obtained as already described, and T the corresponding colour temperature taken from the Greenwich tables. Values of ϕ and T marked with a colon are of slightly less weight, owing to poorer atmospheric conditions, difficulties in measurement or other sources of error.

The values at the beginning of this series overlap in date with the last values of a series determined at Greenwich *, while the later values overlap a series of measurements by Hiltner † at Michigan. The present series thus forms a link between these other published values, and the agreement at the points of overlap is good, both with Greenwich and Michigan.

Gradients and Colour Temperatures of γ Cassiopeiæ

Date	J.D.	ΔG	ϕ	T	Date	J.D.	ΔG	ϕ	T
	2429			°		2429			°
1938 June 20	070	−·04	1·21	13,500	1939 Sept. 3	510	−·44	0·88:	27,000:
,, 30	080	−·10	1·15	14,500	,, 10	517	−·40	0·85	24,300
July 21	101	−·07	1·18	14,000	,, 16	523	−·37	0·88:	22,600:
,, 27	107	−·04	1·21	13,500	,, 24	531	−·41	0·84	25,000
,, 28	108	−·08	1·17	14,200	Nov. 5	573	−·42	0·83	25,400
Aug. 6	117	−·06	1·19	13,800	Dec. 2	600	−·41	0·84	25,000
,, 13	124	−·06	1·19	13,800	1940 Jan. 2	631	−·53	0·72:	37,000:
,, 17	128	−·04	1·21	13,500	,, 18	647	−·46	0·79	29,000
,, 25	136	−·11	1·14	14,700	Mar. 2	691	−·51	0·74	34,000
Oct. 31	203	−·12	1·13	15,000	,, 14	703	−·51	0·74	34,000
Nov. 19	222	−·20	1·05	16,500	Apr. 16	736	−·44	0·81:	27,000:
,, 27	230	−·13	1·12	15,200	,, 30	750	−·43	0·82	26,000
1939 Jan. 1	265	−·21	1·04	16,800	June 5	786	−·37	0·88	22,600
Feb. 16	311	−·27	0·98	18,500	,, 7	788	−·44	0·81	27,000
,, 19	314	−·35	0·90	21,700	July 30	841	−·38	0·87	23,300
Mar. 11	334	−·29	0·97	18,800	Aug. 27	869	−·45	0·80:	28,000:
Apr. 11	365	−·43	0·82	26,000	,, 31	873	−·46	0·79	29,000
,, 14	368	−·42	0·83	25,400	,, 31	873	−·43	0·82	26,000
June 19	434	−·40	0·85	24,300	Sept. 23	896	−·50	0·75	32,500
July 9	454	−·37	0·88	22,600		2430			
,, 22	467	−·41	0·84	25,000	1941 Oct. 23	291	−·45	0·80	28,000
Aug. 1	477	−·36	0·89	22,000	,, 23	291	−·47	0·78	30,000
10	486	−·37	0·88	22,600					

It will be noticed that there was at first a fairly rapid decrease of gradient (increase of T), which continued the drop shown in the diagram of Hunter and Martin, until 1939 April. There was then a sudden change, with a slight average increase followed by a further fall in ϕ to a pronounced minimum in 1940 February, when the temperature reached the exceptionally high value of about 35,000°. Finally there was a rapid gradient increase to a maximum in 1940 July, with an even steeper decline to the end of the series.

These changes were accompanied by pronounced changes in the spectrum. After 1939 April, when the decrease of ϕ was temporarily halted, there was a rapid and very strong increase in the intensities of the central *H* absorption, combined with an increasing separation of the emission components. There was also a sudden reappearance of *He* 3888 absorption, which rapidly became stronger, accompanied by the development of other strong sharp *He* lines, especially of the $2^3p_0 - m^3D$ series, and fading of emission. These changes reached a maximum at about 1940 February, at the time of maximum gradient, and then showed various fluctuations corresponding roughly with the gradient changes. Various other changes were observed, but a detailed description of these is

* Hunter and Martin, *The Observatory*, 62, 237, 1939. † *Ap. J.*, 93, 505, 1941.

reserved for a later paper dealing with the spectrum. The observations recorded above are sufficient to support the principal gradient changes observed, and to justify the following of these in the mean curve (drawn as previously described) for determining probable errors.

An interesting relation between gradient and the number, N, of Balmer lines seen in emission is shown in the diagram. For this purpose the gradient values of the present list are supplemented by those of Greenwich and Michigan (already mentioned) and of Vanderkhove.* The number of emission lines was obtained from the large-scale spectra

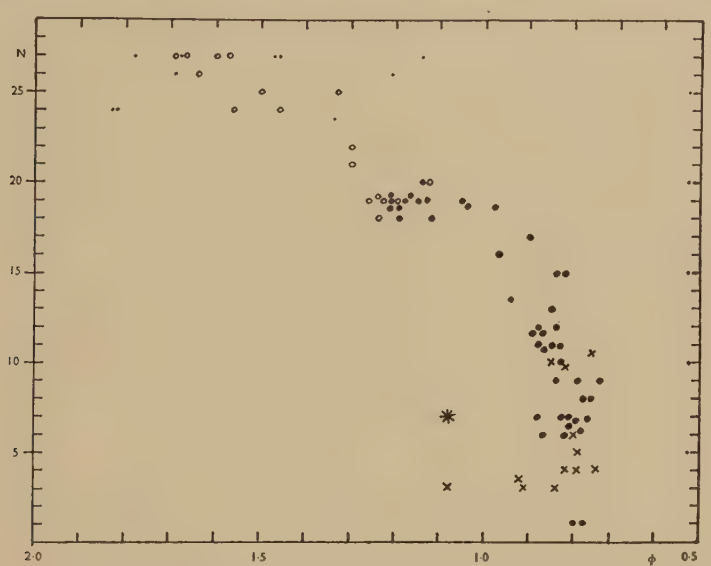

Relation between gradient (ϕ) and number of Balmer emission lines (N).

Open circles = Greenwich ϕ. *Small dots = Vanderkhove ϕ.*
Filled ,, = Edwards ϕ. *Crosses = Hiltner ϕ.*
Asterisk = Pre-outburst.

taken at Sidmouth with the Kensington 9-inch prismatic camera, which gives a good density in the spectrum well beyond the limit of the Balmer series. It has been shown by Greaves and Martin † that in the earlier stages of the outburst in γ Cass an increase of gradient was accompanied by an increase of intensity of the emission lines. Unfortunately the earlier Sidmouth plates were not standardised, so that intensity measures of these could not be made, but the number of lines visible may be taken as a rough indication of the intensity of emission. This number is subject to some uncertainty, but the method is homogeneous throughout the series and there was a considerable number of plates available from which to derive mean values. The probable error of N should be less than ± 1. It will be seen that, with the exception of Vanderkhove's results, there is good correlation between N and ϕ in the upper part of the diagram (from $N=15$ to $N=27$), but in the lower half this condition fails. Here the majority of the points indicate a nearly constant ϕ over a considerable range of N (1 to 15 approximately), whereas some of the Michigan results (seen near the foot of the diagram) show a change of ϕ from 0·8 to 1·1 approximately, with a nearly constant value of N. These changes observed at Michigan are undoubtedly real, as they are much larger than possible errors, and are also supported by the occurrence of spectrum changes.

The points in the diagram follow an approximate time sequence; those at the top being the earliest dates and those at the bottom the latest, though there is some scatter

* *The Observatory*, **62**, 76, 1939. † *M.N.*, **98**, 437, 1938.

in the distribution of dates. It is interesting to note that the point where the correlation between N and ϕ breaks down occurs at 1939 April, when the regular decrease of ϕ stopped and the appearance of a very pronounced "shell" spectrum of strong sharp absorption lines was observed. The change in the relation between N and ϕ might thus be explained by the presence of this shell masking the later emission lines of the Balmer series, or affecting the observed gradient. Such an effect could scarcely, however, account at the same time for the opposite type of variation based on the Michigan values of ϕ, and it seems doubtful if a permanent relation between N and ϕ can be assumed. This is further supported by considering the pre-outburst values. The point marked by an asterisk represents the mean of eleven early Greenwich observations, made in 1926–27. This point lies well clear of both branches of the curve, and it seems that a different law again (if any) must hold for the conditions obtaining at that time.

In conclusion I should like to express my thanks to Mr. D. R. Barber for taking a considerable number of the plates used in this work, and for the use of his atmospheric extinction tables.

Norman Lockyer Observatory,
Sidmouth:
1943 *June* 5.

PHOTOGRAPHIC OBSERVATIONS OF COMETS AT RIVERVIEW COLLEGE OBSERVATORY

D. J. K. O'Connell, S.J.

(Received 1943 June 24)

The plates were taken at Riverview, that of Comet van Gent by P. F. Rheinberger, the remainder by the writer. The instruments used are indicated in the table, A being a $6\frac{3}{4}$-inch Ross lens (f.l. 130 cm.) and G a 4-inch Ross-Grubb-Parsons lens (f.l. 46 cm.). The telescope was guided on the comet, except for the plate of Comet van Gent. In spite of the short focal length of the G lens it was thought worth while to measure the plates, at least by way of experiment, as the lens gives very good images. The plates were measured by the writer on the measuring machine at Mount Stromlo Observatory, by kind permission of Dr. Woolley. The reduction was made by Comrie's method (*J.B.A.A.*, **39**, 203, 1929). Each plate was reduced with two sets of three comparison stars. The results of each solution are given in the table, together with the comparison stars and the respective dependences.

In the lists of comparison stars Abbadia A and B refer to the Abbadia Zones $+5°$ to $-3°$ and $-3°$ to $-9°$, and Yale A, B and C to the Yale Photographic Catalogue $-10°$ to $-14°$, $-14°$ to $-18°$ and $-18°$ to $-20°$ respectively. The star positions were reduced with proper motions when known.

The positions have not been corrected for parallax, aberration or light time.

COMET FINSLER (1937*f*)

U.T.	R.A. (1937·0)		Dec. (1937·0)		Comp. Stars	Dependences			Exp. Min.
1937 d	h m s	s	° ′ ″	″					
Aug. 31·39028	14 06 44·85	44·91	+5 36 28·9	28·8	1, 2, 3	·29593	·40000	·30407	22
		44·79		29·0	4, 5, 6	·38006	·23782	·38212	
Sept. 2·38190	14 07 51·32	51·32	+3 24 35·1	35·2	7, 8, 9	·58603	·13631	·27766	10
		51·32		35·0	7, 10, 3	·62074	·23039	·14887	
Sept. 4·38109	14 08 47·03	47·03	+1 26 56·0	56·4	11, 12, 13	·35360	·12890	·51750	10
		47·02		55·5	14, 15, 16	·49817	·16478	·33705	
Sept. 6·37569	14 09 34·50	34·51	−0 18 13·1	13·2	17, 18, 19	·17533	·63542	·18925	12
		34·49		13·0	17, 18, 20	·10149	·67078	·22773	

Comparison Stars

1. ½ (Pulkowa 56, 4565 +Toulouse 13, 5981).
2. A.G. Leipzig 6629.
3. G.C. 19133.
4. A.G. Leipzig 6616.
5. Toulouse 13, 5988.
6. A.G. Leipzig 6631.
7. G.C. 19103.
8. G.C. 19112.
9. G.C. 19223.
10. G.C. 19233.
11. ½ (Abbadia A 7921 +A.G. Albany 4894).
12. Abbadia A 7944.
13. ½ (Abbadia A 7925 +Yale 3, 4896).
14. G.C. 19141.
15. G.C. 19130.
16. ½ (Abbadia A 7932 +Yale 3, 4901).
17. ½ (Pulkowa 56, 4591 +Yale 5, 3705).
18. G.C. 19188.
19. ½ (Pulkowa 56, 4581 +Yale 5, 3697).
20. ½ (Pulkowa 56, 4582 +Yale 5, 3700).

COMET KOZIK-PELTIER (1939 *a*)

U.T.	R.A. (1939·0)		Dec. (1939·0)		Comp. Stars	Dependences			Exp. Min.
1939 d	h m s	s	° ′ ″	″					
Feb. 16·44028	1 10 00·02	59·98	− 5 59 19·1	19·7	1, 2, 3	·25469	·49933	·24598	4
		00·06		18·5	4, 5, 6	·38047	·20321	·41632	
Feb. 19·41952	1 32 37·64	37·56	−11 21 44·4	44·0	7, 8, 9	·40721	·40584	18695	2
		37·72		44·9	10, 11, 12	·36175	·25210	·38615	
Feb. 19·42892	1 32 41·54	41·50	−11 22 45·2	45·1	7, 8, 9	·41843	·40370	·17787	3
		41·58		45·3	10, 11, 12	·36682	·23850	·39468	
Feb. 21·42153	1 46 37·78	37·74	−14 41 15·1	15·4	13, 14, 15	·16870	·27896	·55234	2
		37·82		14·8	16, 17, 18	·24809	·62443	·12748	
Feb. 23·42222	1 59 41·13	41·11	−17 44 36·4	36·5	19, 20, 21	·25678	·36228	·38094	2
		41·15		36·3	22, 23, 24	·37983	·21889	·40128	

Comparison Stars

1. G.C. 1554.
2. G.C. 1423.
3. ½ (A.G. Strasbourg 278 + Abbadia B 315).
4. G.C. 1463.
5. A.G. Strasbourg 264.
6. G.C. 1493.
7. G.C. 2069.
8. Yale A 313.
9. Yale A 348.
10. Yale A 355.
11. Yale A 331.
12. Yale A 339.
13. Yale B 493.
14. G.C. 2257.
15. G.C. 2172.
16. Yale B 446.
17. Yale B 455A.
18. Yale B 462.
19. G.C. 2569.
20. G.C. 2454.
21. Yale C 527.
22. Yale C 544.
23. Yale C 520.
24. Yale B 533.

COMET CUNNINGHAM (1940 *d*)

U.T.	R.A. (1941·0)		Dec. (1941·0)		Comp. Stars	Dependences			Exp. Min.
1941 d	h m s	s	° ′ ″	″					
Jan. 29·74410	19 42 32·71	32·80	−45 05 29·0	27·5	1, 2, 3	·29875	·42126	·27999	8
		32·61		30·5	4, 5, 6	·38046	·25036	·36918	

Comparison Stars

1. G.C. 27427.
2. G.C. 27577.
3. G.C. 26885.
4. G.C. 27357.
5. G.C. 27167.
6. G.C. 27443.

COMET DE KOCK (1941 *c*)

U.T.	R.A. (1941·0)		Dec. (1941·0)		Comp. Stars	Dependences			Exp Min.
1941 d	h m s	s	° ′ ″	″					
Jan. 25·71493	17 58 22·86	22·86	−53 19 58·8	59·2	1, 2, 3	·22661	·33432	·43907	2
		22·86		58·4	4, 5, 6	·22722	·32034	·45244	
Jan. 25·74965	17 59 45·78	45·88	−53 25 37·8	39·1	1, 2, 3	·24380	·28703	·46917	2
		45·69		36·6	4, 5, 6	·13735	·29379	·56886	
Jan. 29·42332	21 32 24·12	24·17	−54 24 55·3	56·5	7, 8, 9	·20684	·52463	·26853	2
		24·07		54·1	10, 11, 12	·37807	·42055	·20138	
Jan. 31·43333	23 13 31·88	31·88	−44 29 30·6	30·6	13, 14, 15	·03467	·49100	·47433	2
		31·88		30·5	16, 14, 15	·03755	·47942	·48303	
Jan. 31·44410	23 13 56·05	56·14	−44 25 45·4	44·2	16, 17, 18	·51770	·27829	·20401	3
		55·95		46·6	13, 14, 19	·52160	·21568	·26272	
Feb. 7·43264	1 12 09·89	09·88	−13 39 43·4	44·4	20, 21, 22	·25202	·37725	·37073	4
		09·91		42·5	23, 24, 25	·50704	·15243	·34053	
Feb. 7·44346	1 12 13·95	14·03	−13 38 03·9	04·6	20, 21, 22	·25071	·39029	·35900	2
		13·87		03·2	26, 27, 28	·41544	·32473	·25983	

Comparison Stars

1. G.C. 24635.
2. G.C. 24024.
3. G.C. 24906.
4. G.C. 24212.
5. G.C. 24622.
6. La Plata A 6156.
7. G.C. 30720.
8. G.C. 29994.
9. G.C. 30304.
10. G.C. 30521.
11. G.C. 29819.
12. G.C. 30522.
13. G.C. 32260.
14. G.C. 32270.
15. G.C. 32548.
16. G.C. 32184.
17. G.C. 32787.
18. G.C. 32446.
19. G.C. 32836.
20. G.C. 1626.
21. G.C. 1531.
22. Yale B 281.
23. Yale B 327.
24. Yale A 242.
25. G.C. 1439.
26. Yale A 244.
27. G.C. 1725.
28. G.C. 1344.

COMET VAN GENT (1941 *d*)

U.T.	R.A. (1941·0)		Dec. (1941·0)		Comp. Stars		Dependences		Exp. Min.
1941 d	h m s	s	° ′ ″	″					
June 23·51042	15 20 36·65	36·62	−7 32 56·0	56·6	1, 2, 3	·32953	·27830	·39217	10
		36·68		55·4	4, 5, 6	·27103	·41915	·30982	

Comparison Stars

1. G.C. 20636.
2. ½ (Abbadia B 4827 + Pulkowa 56, 4993).
3. G.C. 20588.
4. G.C. 20602.
5. ½ (Abbadia B 4801 + Pulkowa 56, 5483).
6. G.C. 20638.

Notes

Comets Finsler and Kozik-Peltier were observed on instrument A, and the others on instrument G, with the exception of Comet de Kock on January 31 (2 m. exp.) and February 7 (4 m. exp.).

Comet Finsler was very diffuse. The other comets have more or less sharply defined nuclei. On the plate of Comet de Kock of February 7·44346 the images are not good, as the driving clock was giving trouble.